Studies of adhesion by secondary ion mass spectrometry

by A. M. Spool

The study of adhesion requires the characterization of surfaces and interfaces. One surface analytical technique which has been used extensively in the study of adhesion is secondary ion mass spectrometry (SIMS). This paper provides a brief introduction to the basis of this technique and describes the two broad categories of SIMS analyses: static and dynamic. A complete literature review of the applications of SIMS to the study of adhesion follows. The papers reviewed are organized into a series of topics including the nature of surfaces produced by pre-bonding treatments, contamination which produces adhesion loss, polymer damage at interfaces, silanes and adhesion, characterization of polymer/polymer interfaces, and measurements of interface widths by SIMS.

Introduction

A variety of mechanisms can be responsible for the adhesion between two materials. These range from covalent bonding to van der Waals attraction, and include capillary adhesion, electrostatic attraction, and mechanical interlocking [1]. With the possible exception of mechanical interlocking, these mechanisms are each dependent upon the chemistry and composition of the interface. The study of interfacial chemistry and composition and its effects on adhesion requires the use of depth profiling techniques for the analysis of intact interfaces, and of surface analytical techniques for the characterization of pre-bonded surfaces and of surfaces resulting from interfacial failure.

In this paper, the use of secondary ion mass spectrometry (SIMS) for the study of adhesion is reviewed. SIMS can provide both chemical and compositional information about a surface. Like Auger electron spectroscopy (AES) and X-ray photoelectron spectroscopy (XPS), SIMS can be used both in a depth profiling mode and in a surface analytical mode. Unlike those techniques, SIMS analyses are sufficiently different in these two modes as to be optimally performed on two different types of instruments. The paper begins with a brief introduction to SIMS and to the nature of the sputter event, which is the physical basis of the SIMS experiment. The strengths and weaknesses of SIMS are noted, with some comparisons to other characterization methods. The different types of SIMS analyses and the equipment needed are described. A review of the literature follows, organized into topics which pull some unifying themes from the varied papers covered. These include practical attempts to characterize surfaces pre-treated to improve bonding, the analysis of surface contaminants that weaken adhesion, polymer damage at interfaces, studies of silanes

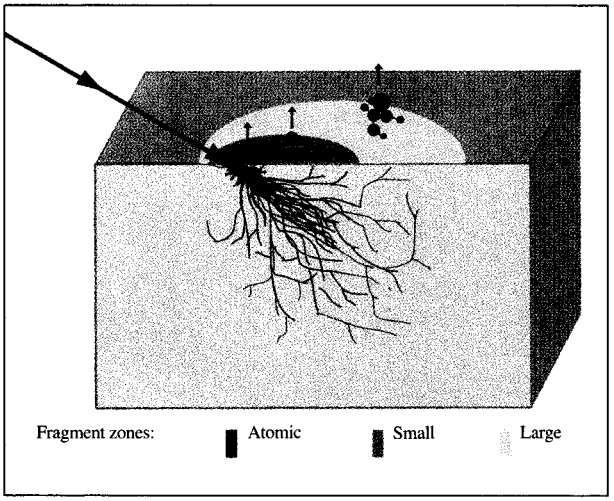

Figure 1

Artist's rendition of the sputter event. Shown is the effect of bombardment of a surface in cross section by a single primary ion. The fragment zones represent a gradient of increasing fragment size with distance from the point of impact. Black lines in the solid represent atomic fragments in motion.

and the mechanisms by which they promote adhesion, characterization of polymer/polymer interfaces, and measurements of interface widths by SIMS.

SIMS

A secondary ion mass spectrometer consists in its simplest form of a primary ion gun, a sample to be analyzed, and a mass spectrometer. The ion gun produces "primary" ions because these initiate the experiment, striking the sample and producing the "secondary" ions which the spectrometer detects. The result of the experiment is a plot of detected counts against a measured mass-to-charge ratio, m/e. In most cases the charge is 1, and the x-axis is typically designated as a mass scale. The SIMS experiment can produce mass spectra with up to six orders of magnitude of dynamic range, so the measured counts may be plotted on either a linear or a logarithmic scale. The large dynamic range, the high probability of ion formation of many species on most surfaces, and the excellent detection efficiency of today's mass spectrometers make SIMS the most sensitive surface analytical technique available today.

The probability of ion formation varies over many orders of magnitude and depends not only on the ionizing species but on the nature of the surface at which it is formed. Under many circumstances, the quantification of SIMS data remains difficult. By comparison, AES and XPS spectra are much more readily quantified.

Peaks in SIMS spectra are due to atomic ions, inorganic cluster ions, organic fragment ions, and molecular ions. As a result, SIMS spectra contain information about both the atomic composition of surfaces and the bonding (chemistry) present at the surface. The presence of molecular ions and fragments in these spectra is particularly important for the identification and characterization of organics at surfaces. For organics, AES line shapes and XPS binding energies may provide some information about the types of organics present (aliphatic, aromatic, etc.), but organic species cannot be directly identified using these techniques.

Because mass is measured in the SIMS experiment, isotopes of the elements are readily distinguished. Isotopic labeling in conjunction with SIMS provides avenues of inquiry not possible with AES and XPS.

The high sensitivity of SIMS creates the potential for imaging. Modern liquid metal ion guns have spot sizes as low as 50 nm. Excellent mass resolved images can be obtained. The lateral resolution possible with a 50-nm beam does not equal that available in AES, but the sensitivity allows images to be collected in a fraction of the AES acquisition time. XPS images, while now becoming common, have less lateral resolution and require long acquisition times.

The unique information SIMS provides, and the way it complements other surface analytical tools, have made it an increasingly important technique for the study of adhesion [2–9]. SIMS is an excellent technique for the study of the effects of pre-treatments, etchants, and cleaning methods on surfaces to be bonded. Its sensitivity allows the detection of trace elements that sometimes accompany these processes. Its specificity allows the direct identification of unwanted organic contaminants. SIMS is a sensitive probe for oxide layers. Isotopic labeling experiments in conjunction with SIMS can help determine adhesion failure mechanisms and the mechanisms by which polymers adhere.

SIMS may also provide results that are equally well obtained by AES and by XPS. SIMS may have been used in some of the work reviewed here because of the greater speed of analysis.

The interpretation of SIMS data is often less direct than that of AES or XPS data. Varying peak intensities may indicate varying ionization probabilities as well as varying concentrations. Cluster ions may indicate bonding at the sample or recombination above it. The interpretation of the data produced in a SIMS experiment begins with an understanding of the process in which the secondary ions being measured are formed.

- *The sputter event*

When an ion with an energy of several keV strikes a surface, it penetrates into the sample and starts a collision

cascade. Some few displaced atoms from the cascade reach the surface and cause a portion of the surface to be ejected (sputtered). A fraction of the sputtered material retains a charge and is readily detected by the mass spectrometer. An example of a typical collision cascade [10–13] is shown in **Figure 1**. This cascade has been successfully modeled as an elastic process [10]. The initial collision of the primary ion with the surface results in atoms being driven in all directions. Close to the area of impact, atoms moving toward the surface arrive with high energies, and produce sputtered atoms and mononuclear ions. Some of these atoms and ions may recombine above the surface to form multi-atom clusters. In the direct area of impact, at 10^{-12} s after the primary ion strikes the surface, most atoms will be in motion. The resulting sudden loss of atoms and ions from the surface is called "thermal" sputtering. Finally, since the collision cascade extends some distance from the impact site, the moving atoms reach the surface with much lower energies. Occasionally they do so with just enough energy to desorb whole molecules or sections of the surface. Large polymer fragments and large intact inorganic clusters originate at these distances (10–20 nm) from the original point of impact.

The cascade extends 10–25 nm into the solid (depending on primary ion energy, mass, and the composition of the surface it strikes), while most ion emission occurs from the top few monolayers. Depending on the probabilities of ionization, and neutralization by electrons from conductive sample surfaces, many ion impacts (and resulting cascades) may occur before a single ion is formed that escapes to be analyzed by the spectrometer. Even though recombination may heal many of the defects created by a cascade, significant damage to the near-surface region occurs even before sputtering has removed a single monolayer from a surface. If the surface is an insulator, and especially where it consists of organic species, recombination is less effective, and the damage is more extensive. **Figure 2** demonstrates the effect the cascade has on SIMS spectra. Figure 2(a) is the SIMS spectrum of the surface of a silicon wafer with photoresist and polydimethylsiloxane contamination, analyzed using a minimum ion dose ($<10^{12}$ ions/cm^2). This dose, less than the "static" limit (see below), damages only a small fraction of the surface (<0.1% of a monolayer, just enough to analyze) and is insufficient to sputter a significant portion of the surface. After brief dc sputtering [Figure 2(b)], sufficient to remove only ≈10% of a monolayer, many large molecular fragments of the siloxane contaminant are no longer detected, and the "fingerprint" low-mass spectrum which matched that of the photoresist is altered beyond recognition. After sputter removal of ≈1 monolayer [Figure 2(c)], virtually all molecular information is gone.

The collision cascade process makes spectra of samples which have been sputter-etched remarkably different from

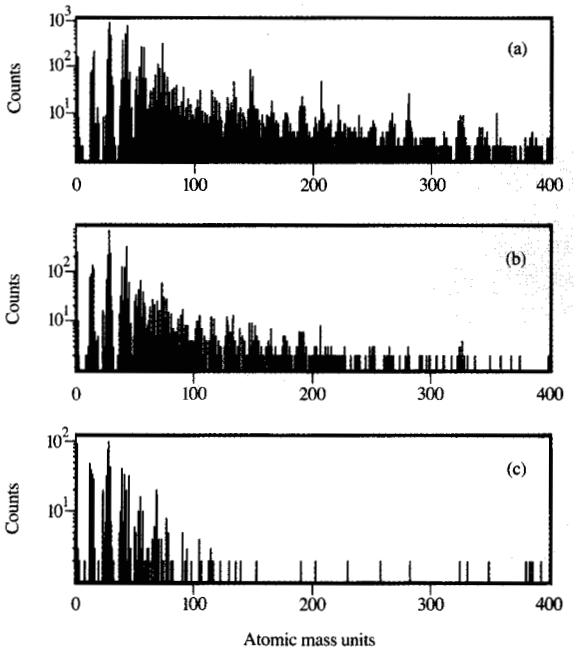

Figure 2

Effect of the collision cascade on SIMS spectra when the static limit is exceeded. (a) Static SIMS spectrum obtained in a Charles Evans and Associates TOF–SIMS instrument using a 25-keV Ga^+ primary ion source of a photoresist surface as received. In addition to signals from the photoresist, the spectrum shows evidence of contamination by polydimethylsiloxane. (b) Static SIMS spectrum of the same surface after a 60-s sputter with a 60-pA 25-keV Ga^+ ion beam rastered into a 117-μm-wide square. Estimated material removed is approximately 0.1 monolayer. (c) Static SIMS spectrum of the same surface after an additional 85-s sputter with a 500-pA 25-keV Ga^+ ion beam rastered into a 117-μm-wide square. Estimated material removed is 1 monolayer.

spectra of unetched surfaces. The static SIMS limit is defined as the ion dose at which an alteration of the surface becomes apparent in the SIMS spectrum. Below that limit, the probability of a primary ion striking a spot on the surface already damaged by a previous ion is not significant. The maximum dose for a static SIMS experiment is typically between 10^{12} and 10^{13} ions/cm^2. The dose varies because the area of the sample damaged by an ion impact differs from sample to sample, from ion to ion, and with ion energy and angle of incidence.

The static SIMS limit leads to a natural distinction between modes of SIMS operation. Static SIMS is the mode in which exposed surfaces may be analyzed unaffected by the ion beam. Dynamic SIMS is the mode in which the surface is intentionally etched, typically for

the purpose of producing a depth profile. In some early work with less sensitive spectrometers and before the importance of the static limit was realized, analyses were reported during which the samples were unintentionally damaged. This mode of operation has sometimes been referred to as quasistatic SIMS.

• *Static SIMS*

The use of static SIMS as a standard analysis tool is a recent development. Static SIMS analysis of the exposed surfaces from failed interfaces is often successful in determining the chemistry and composition of the failure site. In particular, the question of whether failure was interfacial or cohesive (within one of the materials) in nature or involved a weak transition layer can often be resolved through the use of static SIMS. In this situation, static SIMS may be preferred because it has a significantly shallower analysis depth (1–2 monolayers) than either AES (2–3 nm) or XPS (3–6 nm). Especially when a contaminant or altered layer is organic, the molecular information available in the static SIMS experiment is invaluable. Quantification at a chemically unique interface is difficult given surface-dependent variations in ion yields. Comparisons between similar surfaces, however (varying only, for example, in the degree of bondability), can produce accurate relative compositions.

The time-of-flight (TOF) spectrometer is ideal for the static SIMS measurement: It can detect as much as 50% of the ions generated at the sample during the analysis. In this type of spectrometer, the primary ion gun is pulsed. The secondary ions formed are accelerated to a uniform energy, and are separated in mass by their time of arrival at the detector. The current in the initial primary ion pulse is set low enough that all of the ions that reach the detector can be individually counted. As a result, damage to the sample during spectrum acquisition is minimized. Modern TOF spectrometers are capable of high (10 000 $m/\Delta m$) mass resolution. Coupled with ion guns that can produce subnanosecond pulses, the TOF spectrometer can resolve most ions, even those at the same nominal mass.

In contrast, the two other major spectrometer types used for SIMS must scan during spectrum acquisition. The oscillating potentials on the four rods used in the quadrupole mass filter are set to allow ions of only a given m/e to pass through to the detector. This potential must be scanned to produce a complete spectrum. Similarly, the fields in the magnetic sector instrument must be scanned to successively detect all of the ions in a spectrum. While the quadrupole or magnetic sector is selecting ions of a given mass, all other ions are deflected toward the spectrometer walls and are not detected. Because of this inefficiency, static SIMS spectra obtained using these spectrometers must be acquired from a large area of a sample to keep the total dose below the static limit.

Early surface analyses by SIMS were almost invariably quasistatic. Molecular information in these spectra was limited or nonexistent. Nonetheless, the elemental and small-fragment ions detected were characteristic of the original surface. Quasistatic SIMS analyses revealed a good deal of information about adhesion under what would now be considered less than ideal experimental conditions.

• *Dynamic SIMS*

Dynamic SIMS has been developed largely as a technique for the semiconductor industry. Its sensitivity, quick turnaround, and ability to quantitatively measure ion implants drove the industry acceptance of this analytical tool. Dynamic SIMS can readily quantify a small concentration of an element found in an otherwise known and well-characterized solid such as silicon. SIMS depth profiles can be used to locate isotopes used in labeling experiments. Interpretation of dynamic SIMS depth profiles becomes more difficult when interfaces are involved. Sputter yields and ionization probabilities can vary greatly at an interface from their values in either of the joined materials. Oxygen present at an interface tends to dramatically increase positive ion yields (by reducing the rate of electron transfer from the surface that neutralizes secondary ions). Nonetheless, comparisons between dynamic SIMS depth profiles of similar samples provide important information about composition differences at interfaces. A pertinent example is the comparison of a sample with strong adhesion at an interface to one with a weak interface. Sputter depth profiles provide information about thin-film thicknesses. Where the width of an interface in a depth profile exceeds the expected depth resolution (and especially where a similar sample demonstrates a much sharper interface), conclusions can be drawn about interface roughness, interlayer diffusion, or the formation of boundary layers. Because of the shallow analysis depth of SIMS relative to AES and XPS, dynamic SIMS profiles can potentially yield better depth resolution.

During depth profiling, the damage to the sample caused by the sputter event after a few monolayers are removed leaves only a simple, mostly atomic, mass spectrum. Energy filters may be used to select the higher-energy atomic species in order to further reduce molecular interferences. When a spectrometer with high mass resolution is available, atomic species can be resolved from molecular or cluster fragments. Unfortunately, the cascade will also blur an interface well before it reaches the surface, thereby limiting depth resolution. Sputter-induced broadening is encountered in all sputter profiling techniques including AES and XPS.

The ideal spectrometer for most dynamic SIMS measurements is a magnetic sector instrument. Typically, only a few ions are selected for analysis in a depth profile.

As a consequence, the handicap encountered by the sector instrument in obtaining static SIMS spectra is for the most part removed; little scanning is required during depth profile acquisition. Compared to normal sector instruments (such as those used with gas chromatography mass spectrometry, GCMS), a wide magnet bore is used to improve the transmission of ions with a wide distribution of emission angles. Transmission of ions of a selected mass may reach 30%. There is a trade-off in the operation of a sector instrument between mass resolution and transmission efficiency. High mass resolution is available to resolve species with similar masses, but the price is reduced sensitivity.

A less expensive option is a quadrupole mass filter. With lower transmission (less sensitivity) and lower mass resolution, this spectrometer can nonetheless provide reasonable sensitivities in depth profiling. As with the magnetic sector instruments, scanning is minimized during typical depth profile acquisitions.

The TOF spectrometer is not ideal for dynamic SIMS because it cannot analyze during a dc sputter etch. Under the conditions in which most TOF–SIMS instruments are used, it is not possible to etch material from the sample using a pulsed primary gun at a rate that would allow depth profiles of any but the thinnest layers. Secondary ions produced during the dc etch are lost, and overall sensitivity is reduced. Recent work [14] has explored the use of TOF–SIMS for shallow depth profiles where relatively little dc sputtering is required. The advantage of the TOF in this context is in profiling for unknowns, since the spectrometer is not scanned and the entire mass spectrum is available at each profile depth for which data are taken.

Review of SIMS adhesion studies

The following sections review the use of SIMS in the study of adhesion. The first section, on pre-bonded surfaces and adhesion, contains subtopics on contamination, polymer modification, and the use of silanes to promote adhesion. Subsequent sections cover silanes, polymer interfaces, and measurements of interface widths. Many of the approaches described have become routine in the industrial environment.

- *Pre-bonded surfaces and adhesion*

The state of a surface to be bonded has a direct effect on bond strength. The following section reviews the use of SIMS to characterize surfaces prior to bonding and the effects pre-bonding treatments have on them. The relationship between the state of the original surface and adhesion strength is explored.

The effects of pre-bonding treatments on the surface of AISI 304 stainless steel were determined using a combination of scanning electron microscopy (SEM), XPS, and dynamic SIMS [15]. These surfaces were subsequently bonded with epoxy. The differently treated steel surfaces varied in bond durability and strength as measured using a wet peel test and a shear test after aging (750 h, 70°C, 98% RH). Surfaces anodized in nitric acid or sulfuric–chromic acid produce superior bonds. SIMS depth profiles, calibrated using SEM measurements on the thickest films, were used to determine oxide layer thicknesses. The superior surfaces had oxide layers with thicknesses between 46 and 66 nm. With the exception of one film with a very thick oxide (250 nm), all other treatments produced oxide films less than 10 nm thick. SEM photographs (not included here) showed that the surfaces with the best bonds had oxide films that were porous in nature, while oxides on the other surfaces were not porous. The results are consistent with the hypothesis that the best surfaces are those with oxide films that can mechanically interlock with the epoxy.

The adhesion stability of lacquered aluminum foil used for packaging applications can be undermined by the degreasing annealing process used on the foil [16]. The process is intended only to remove hydrocarbon oil residues from the foil. Improperly controlled, this process can also cause segregation of Li and Mg, impurities in the bulk, to the surface. Surface coverage of magnesium was determined by integrating SIMS depth profiles (Mg was located throughout the oxide, which has some depth). Depth profiles were obtained from foils annealed at three different temperatures and for varying times (**Figure 3**).

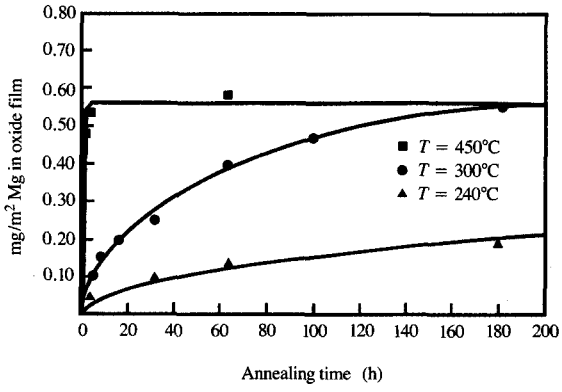

Figure 3

Magnesium surface coverage determined by integration of quantitative SIMS depth profiles as a function of annealing time at temperatures of 240, 300, and 450°C. Commercial Al 99.2 foil, 40 μm thick, bulk Mg concentration 11 ppm. From [16], reproduced with permission.

Assuming that diffusion of Mg to the surface is the rate-determining step, a model was developed that fits the experimental measurements. Diffusion coefficients calculated from these data were in turn found to be a function of the aluminum grain size. This information was used to control the annealing process and avoid Mg-induced lacquer adhesion loss. Older quasistatic SIMS results showed that, alternatively, an additional deoxidizing treatment of the aluminum can be used to remove the surface-segregated Mg [2].

A recent paper explored the effects on a steel surface of a replacement for the older degreasing annealing process: cleaning the foil in an aqueous solution of Na_3PO_4, $NaCO_3$, and surfactants [17]. Static SIMS and XPS measurements were used to monitor the composition of the surface as a function of cleaning time. After 30 s, the hydrocarbon oil is completely removed. Over the next minute, the Mg level continues to decline, and over the next few minutes, P, Fe, and Cr levels increase. The deposited P, undetected by XPS, is of interest because PO_4^{-3} is known to promote adhesion on aluminum and steel substrates. SEM photographs show that the continued loss of Mg is accompanied by roughening of the surface. The surface roughening is also expected to promote adhesion.

A quasistatic-SIMS (and ion scattering spectroscopy, ISS) study of a Ti_6Al_4V alloy surface after a pre-bonding etch (aqueous solution of HF acid and $NH_4H_2PO_4$) shows, after the initial cleaning effects, continued V enrichment of the surface and a concomitant decrease in surface Al [18]. The etchant roughens the surface, but continued etching only has subtle effects on the surface topography, while adhesion continues to be enhanced. Adhesion was measured for an evaporated gold film and a commercial adhesive by both a tape peel test and lap shear tests. Adhesion could be degraded by oxidation of the surface (pre-bonding treatment with steam, which also contaminates the surface) and by heating the surface in air. In both cases, weak oxides contaminated with alkali metals were found at the failed interface.

The effectiveness of oxide removal by an *in vacuo* reactive ion etch (RIE) of polysilicon prior to chemical vapor deposition (CVD) of tungsten silicide was determined by dynamic SIMS [19]. The presence of the oxide causes adhesion loss during high-temperature annealing or oxidation processes. The RIE etch chosen using C_2F_6 left an unquantified amount of fluorocarbon residue at the interface, but while attempts to eliminate this contaminant failed, this material did not affect adhesion or device properties. While the resulting decrease in oxygen at the interface could be confirmed using AES, dynamic SIMS was required to show the nearly two-orders-of-magnitude decrease in the oxygen level.

The dependence of adhesion strength (measured by scratch, peel, and ultrasonic tests) on the oxygen content of the interface between evaporated aluminum layers and polyethylene terephthalate (PET) films was determined using dynamic SIMS [20–22]. The studies independently noted the presence of a base level of oxygen at the interface, most likely due to oxygen originally present on the PET surface. The effects of both aluminum deposition rate and residual gas pressure during deposition on the subsequent adhesion strength of the aluminum layer were measured [20] by scratch and peel tests. An optimum oxygen level was noted. The results are consistent with the hypothesis that in the absence of other oxygen, oxygen on the PET is gettered by the growing aluminum layer. It follows that the optimum conditions exist when there is enough residual oxygen pressure during deposition to prevent gettering of the surface oxygen and allow C–O–Al bonds to form. If the residual oxygen pressure is too high, the aluminum grain size is reduced, and stress increases in the film. A relationship between bulk oxygen content and grain size was demonstrated with a combination of dynamic SIMS and transmission electron microscopy (TEM). Because aluminum oxide is sputtered at a much slower rate than aluminum, the sputter time through films of identical thickness was also an indicator of the level of oxygen in the bulk aluminum layer and, consequently, the grain size [21]. PET films with different levels of crystallinity donate different amounts of oxygen to the growing aluminum layer and can alter adhesion strength by a factor of two [22]. The PET sample with high crystallinity donates more oxygen to the Al film (thereby reducing the Al grain size) and less to the interface than the PET with low crystallinity. The SIMS profile also shows that the coated PET sample with high crystallinity has a wider interface and a greater adhesion strength (peel test).

PMMA is the substrate onto which silver is plated by an electroless process for use in optical disks (laser disks for video applications) [23]. To initiate this reaction, tin must be present on the PMMA surface. Treatment of the PMMA with tannic acid is essential to fix stannous ions to the surface. Other spectroscopic techniques, including XPS, had not previously detected tannic acid on the treated surface. Static SIMS analysis clearly identified tannic acid on the treated PMMA. This result shows that it is the presence of tannic acid which allows the surface to bind the stannous ions necessary for silver plating.

An alumina surface must be cleaned and prepared for electroless deposition of nickel [24]. The surface was analyzed with static SIMS and X-ray fluorescence spectrometry (XRF) before each of the cleaning, etching, sensitization, intermediate, and activation steps performed prior to nickel plating. The cleaning step removes organics, magnesium, and calcium from the surface. Static SIMS spectra reveal traces of the surfactant that remain after this step. Etching in HF removes silicon and Na but leaves F,

even after the rinse. The sensitization step, which uses $SnCl_2$, predictably leaves Sn on the surface, detected by SIMS as Sn^+ and tin oxide fragments, and by XRF. Cl also remains on the surface (but is not detected by XRF). The intermediate step, in which the alumina is treated with a solution of $AgNO_3$, leaves the Sn^+ signal unchanged, and adds Ag^+ to the SIMS spectrum and Ag to the XRF findings. Only after the activation step with $PdCl_2$ do complexes of Ag with Cl appear in the SIMS spectra. Pd and Cl are now detected by both SIMS and XRF. The SIMS and XRF signals for Sn and Ag remain unchanged. The Pd deposited on the surface in this way provides catalytic nucleation sites for electroless plating. The authors propose a mechanism for this overall surface activation process in which Sn reduces $AgNO_3$ to surface-bound metallic Ag, which in turn reduces the Pd^{+2} to surface-bound metallic Pd. Sn and Ag remain on the surface as salt precipitates.

The adhesion between the resulting electroless Ni layers and the alumina is weak. In order to better understand this interface, recent work included adhesion measurements by direct pull tests and by 90° peel tests (which are proportional to the adhesion strength and fracture energy, respectively) [25]. Interface and fracture surface analyses were performed using SEM with energy-dispersive X-ray analysis (EDX) [25], TEM, AES, XPS, and static SIMS [26]. For these studies, Ni layers were deposited using two different electroless Ni(P) plating solutions [25]. One solution contained glycine as the complexing agent, and the other, acetate. Two alumina substrate types with different roughnesses were used. The mechanical measurements showed that Ni films deposited using glycine have an adhesion strength much higher, and a fracture energy lower, than Ni films deposited with acetate, regardless of substrate type. The inverse relationship between these two measurements shows that the interfacial chemistry alone cannot explain these results. The high adhesion strength measured on smooth substrates does suggest that the chemistry of the interface contributes to the adhesion. The analytical studies bear this out [26]. Cross-section TEM analysis shows good interfacial contact for all of the Ni films measured, along with a 1–2 nm interfacial layer. The XPS and SIMS results show that failure occurs in this interfacial layer. For both techniques, spectra of the Ni layer fracture surfaces and of the Al_2O_3 fracture surfaces show strong signals due to the respective substrates. Ni- and P-containing ions are detected by static SIMS on the alumina fracture surfaces in all cases, but Al-containing ions are detected on the Ni layer fracture surfaces only when the alumina ceramic used is rough. Sn, Ag, and Pd are detected on the Ni side of the fracture, but only Sn is detected on the Al_2O_3 side. Ion fragments which indicate the presence of glycine and acetate are found in spectra of the fracture surfaces of samples plated from the glycine- and acetate-containing solutions, respectively. SIMS spectra of a sample peeled *in vacuo* did not show the other organic fragments found in the spectra of air-exposed fracture surfaces. All of these results are consistent with the probability that a thin layer of plating solution remains at the interface after deposition of the Ni layer. Consistent with this hypothesis is the fact that adhesion of plated Ni layers to smooth substrates improves if the sample is dried between the deposition of the first 0.1 μm and the deposition of the rest of the film.

Surface analysis of fracture surfaces can help determine adhesion or failure mechanisms and thereby influence the choice of prebonding treatments. Early quasistatic SIMS and ISS analyses of the fracture surfaces of two epoxy/metal bonds showed that lap-shear-induced adhesion failure occurred at the epoxy/metal interface [27]. The samples consisted of an anodized Ti surface bonded to a magnesium-silicate-filled epoxy and an aluminum surface bonded to a TiO_2-filled epoxy. The epoxy fillers essentially labeled the epoxy for quasistatic SIMS and ISS analysis. As in the case described above for the electroless Ni layer bound to the rough alumina substrate, elements of both substrates (i.e., epoxy and metal) were found on both of the fracture surfaces. During interface failure, interlocking pieces of epoxy and aluminum break off to remain attached to the opposite surfaces. These results demonstrate that mechanical interlocking plays a role in the adhesion at these interfaces.

Zinc phosphate conversion coatings produce better adhesion of paints to metals. Dynamic SIMS and SEM were applied to the study of corrosion-induced paint de-adhesion on zinc-phosphated steel [28]. The results show an intact layer containing Zn, P, and Fe (the conversion coating) between the paint and the steel in unaffected regions, but dissolution of this layer where corrosion had induced loss of adhesion of the paint.

Contamination and adhesion

A lack of surface cleanliness is the bane of adhesion. The assessment, identification, and control of surface contamination is an important application of static SIMS. The technique can simultaneously monitor inorganic and organic species. Organic contamination can be identified in many cases. Because the analysis is nondestructive, static SIMS is often the first technique applied to the analysis of a contamination-related adhesion problem.

Studies of the effective removal of hydrocarbon oils from aluminum foils have been described above in the context of a degreasing annealing surface pre-treatment [2, 16, 17]. Both the hydrocarbons and the Mg and Li that segregated to the surface from the bulk are examples of contaminants whose identification and control were made possible through the use of SIMS.

An early review of quasistatic SIMS and ISS analyses of contaminated metal surfaces [3] describes the then already routine use of SIMS in the industrial laboratory for contamination analysis of pre-bonded surfaces. SIMS was used, not only to monitor the effectiveness of various cleaning processes, but to identify those cleaning reagents that end up incorporated into the surface. B and P, for example, are detected on Al surfaces which have been cleaned using boric and phosphoric acids. Recontamination of the Al surface occurs readily upon contact with some gloves and papers. Peel-strength-measured adhesion is reduced by 30–50% in areas of the Al where the contact occurred. ISS and SIMS readily detect the transferred organic contaminants responsible for the adhesion strength loss.

Some of the most common adhesion-destroying contaminants, polydimethylsiloxanes (PDMS, also known as methylsilicones), have distinct mass spectra and are easily detected by static SIMS. Silicone rubber will outgas silicones. Silicones are used as mold-release agents, as stress-cracking agents for low-density polyethylene (LDPE), and as controlled-release additives [29]. Some vacuum greases are composed of silicones (Dow Corning 710 uses a variant, phenylmethylpolysiloxane). The uses are legion. Droplets of silicone oils have been mapped on LDPE and have been linked to localized adhesion loss for coatings and ink [6]. Static SIMS analysis of the fracture interface in an alloy epoxide composite system in one study showed the distinct presence of silicones [30]. The authors noted that contamination levels at or below the detection limits of XPS and AES were sufficient to be associated with adhesion failures. In this laboratory and elsewhere [31], independent analyses have shown that silicones inhibit ultrasonic wire bonding to electroplated gold pads. The sensitivity of SIMS for these compounds is so great that they are detectable at concentrations well below that which causes adhesion loss.

The source of contamination responsible for adhesion loss may be intrinsic to a system. One example of segregation to the surface of Mg and Li impurities in Al foil was described above [2, 16, 17]. Another involves the lead used as a grain-refining agent in some gold plating baths [31]. Segregation of the lead to the gold surface impedes ultrasonic wire bonding. This is true, even in some instances when the lead is present in concentrations below the detection limit of standard XPS. Examples of intrinsic organic contaminants are the anionic surfactants used in coalesced acrylic latex films [32]. The surfactants are used to stabilize water-based colloidal dispersions of polymer particles. The particles coalesce when the latex dries. Static SIMS measurements show that the sodium dodecylsulphate and sodium dodecyldiphenylethersulphonate surfactants segregate to both the air and substrate interfaces.

The study of the causes of localized delamination of the sputtered layers on magnetic recording disks has been an ongoing effort in this laboratory. Depth profiling techniques such as AES or dynamic SIMS may help determine what is different about the interface in these regions. This is especially true if the cause of delamination is inorganic in nature (a chemical change in the substrate at that point or an inorganic contaminant). These techniques are inadequate to the task if an organic contaminant is responsible for the delamination. Defects only a few microns in diameter cannot be mechanically opened for surface analysis, and sputter etching destroys any molecular information likely to help in the identification of the contaminant.

Laser ionization mass analysis (LIMA) is a tool that can sometimes be helpful in these situations [33]. Laser ablation both produces ions for analysis and erodes the surface. The analysis, typically using a time-of-flight mass spectrometer, is compatible with TOF–SIMS; both are readily accommodated in the same instrument. The mechanism of erosion is not of necessity as destructive as that of sputtering. Thermally stable nonvolatile species present at a buried interface survive the ablation process. However, LIMA is less sensitive than SIMS and thus can miss a thin layer at a buried interface. Laser pulse variability is often reflected in major spectrum variations, which can make spectral identification of unknowns difficult.

Laser ablation experiments on disk defects show that the thermal shock brought about by even relatively weak laser pulses (normally below that needed to produce ions for analysis from a thin-film magnetic recording disk) often opens closed defects.* The delaminated sputtered layers of the defects are removed by the laser pulse, exposing the substrate surfaces to which the films had not adhered, or had adhered only weakly. Subsequent LIMA analysis is occasionally but inconsistently useful for the reasons described above. Static SIMS analyses of the exposed substrate are more useful. Similar and related defects, after being opened with the laser, give similar spectra. The spectra often provide a direct analysis of the contaminant responsible for the formation of the defect.

Figure 4 shows ion maps obtained during static SIMS analysis of a circular magnetic recording disk delamination defect, approximately 140 μm in diameter. Cracks in the sputtered layers, visible optically, are highlighted by a map of Co [Figure 4(b)]. In a few small locations, the cracks are wide enough to allow nickel ions from an electroless-nickel-plated substrate to be detected [Figure 4(e)]. Streaks which are also visible optically, the result of the scraping of the top of the defect by a magnetic recording head, are mapped best by ion fragments of the fluoroether

*A. M. Spool, unpublished results.

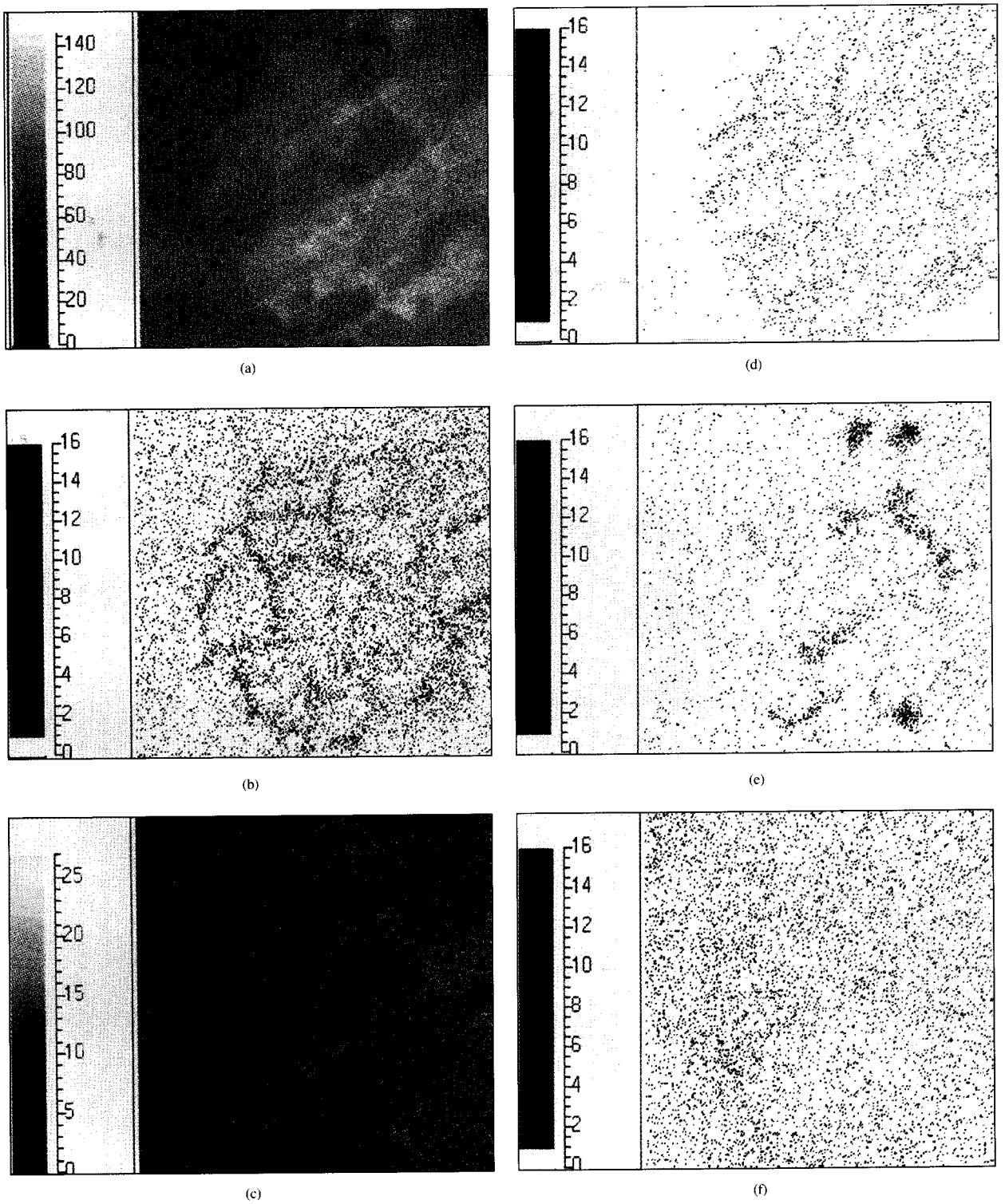

Figure 4

Mass-selected positive ion images of a thin-film magnetic recording disk delamination defect obtained using the microprobe mode of the Charles Evans and Associates TOF–SIMS using a 25-keV LMIG Ga^+ source. Images represent an area approximately 150 μm across. Scale to left gives the color code for counts in a pixel. (a) Total positive ion image. (b) Co^+ image. (c) $C_2F_5^+$ image (fluoroether lubricant). (d) Cr^+ image. (e) Ni^+ image. (f) $C_4H_9^+$ image.

lubricant [e.g., C_2F_5 peak, Figure 4(c)]. Laser ablation was performed using a NdYg laser quadrupled to 266 nm. The laser spot size was less than 5 μm. Laser power was adjusted so as to cause a barely discernible optical effect on an area of the sample away from the defect. Ion maps showing the effect of a laser pulse on the defect are found in **Figure 5**. In the total ion image [Figure 5(a)], a dark area can be seen where the laser has removed a section of the defect surface. The reason the total ion yield is so reduced in this region is that the fluoroether lubricant, which has a high ion yield, has been removed with the delaminated layers [Figure 5(c)]. Some Cr from the first of the sputtered layers has remained behind after the ablation step [Figure 5(d)]. Ni from the underlying substrate remains covered by the contaminant and residual Cr [Figure 5(e)]. Figure 5(f) shows the map of the $C_4H_9^+$ ion. The map clearly shows that a hydrocarbon contaminant remains at the interface after the ablation step. A spectrum of the exposed substrate has major peaks at 27, 41, 57, 69, 83, and 97 amu. Accurate mass analyses of these peaks show that they are due respectively to the $C_2H_3^+$, $C_3H_5^+$, $C_4H_9^+$, $C_5H_9^+$, $C_6H_{11}^+$, and $C_7H_{13}^+$ ion fragments. This specific and reproducible mass spectrum identifies the contaminant as a hydrocarbon oil found on the manufacturing line in a tool used during the preparation of thin-film magnetic recording disk substrates.

Polymer damage and adhesion

Polymers may be intentionally or unintentionally altered by pre-bonding treatments, or by the process by which metal layers are deposited.

The effects of solvent wiping of polypropylene (PP) were studied using static SIMS [34]. This wiping is followed by the application of a chlorinated polypropylene (Cl–PP), which promotes bonding of paint to the poorly wettable PP surface. Static SIMS spectra taken before and after wiping show that only one solvent tested, a mixture of isopropyl alcohol and low-boiling-point aliphatics, had a significant effect on clean polypropylene surfaces. The spectra indicate that hydroxyl groups are introduced to the surface after wiping. The authors speculate that the hydroxyl groups can improve wettability of the surface through hydrogen bonding to the Cl atoms in the Cl–PP primer. The behaviors of grade A (rubber-toughened) PP and grade B (rubber-filled) PP differed when bonded in this fashion. When grade A PP is used, the hydrogen bonding model fully accounts for the enhanced adhesion. Peel-test-induced failure of this interface occurs between the Cl–PP primer and the PP substrate. SIMS and XPS spectra show the presence of Cl only on the paint side of the fracture. Failure occurs in an interphase when grade B PP is used. Spectra from both sides of the interface are identical and show the presence of a mixture of Cl–PP primer and PP. This result suggests that the two polymers have codiffused to form the interphase. This conclusion is substantiated by quantitative XPS analysis of Cl levels of interphase layers formed from primer layers of different thicknesses. These analyses suggest dilution of the Cl–PP by PP. Not surprisingly, the grade B PP, which has a rubber filler with greater chain mobility, produces more highly diluted primer layers, and thus produces a stronger bond.

Modifications of polymethylmethacrylate (PMMA) by ion beams [35], UV light in an argon atmosphere [36], and plasma treatment [37, 38] have been studied by static SIMS. These treatments can enhance metal adhesion or reduce unwanted adhesion in biological systems to PMMA. Low doses of 4-keV Xe^+ ions ($\simeq 10^{13}$ ions/cm^2) actually result in an increase in prominent peaks in the SIMS PMMA spectra. These peak intensities then decrease, along with the total secondary ion count, with increasing ion doses [35]. For those peaks representing major fragments of the polymer (e.g., $CH_3OOCC(CH_3)CHC(CH_3)COOCH_3^-$ at 185 amu), the intensity increase comes at very low ion doses where chain scission occurs, making fragmentation from chain ends more probable. The effects of higher doses are those expected from the collision cascade (see above). For the cyclic tropyllium ion ($C_7H_7^+$), the maximum intensity in the SIMS spectra is reached at much higher ion doses. This ion forms from aromatic rings and long unsaturated chains from which the carbonyl group has been removed, structures formed only as the result of significant damage. Similarly, other ions which form from highly damaged regions of the polymer also peak at these higher doses. Further crosslinking reduces the probability of forming any ion fragments. The above analysis implies that the carboxyl groups are lost with ion bombardment, and indeed static SIMS measures a decrease in the O:C ratio with increasing ion doses. UV radiation induces many of the same effects on PMMA, but in addition, there are signs of surface oxidation not present in the spectra of ion-bombarded PMMA [36]. In contrast, plasma treatment degrades the polymer through main chain scission, leaving a surface distinct from either of the other two treatments [37, 38].

The changes in the surface of polyimide (PMDA–ODA) brought about by an argon plasma (60 Hz, 40 V, 200 mbar) were studied using static SIMS [39]. The treatment improves the hydrophilicity and thereby the bondability of this surface. Polyimide, like PMMA, is degraded by plasma treatment through chain scission. Nitrogen-containing fragment ions with peaks at 28, 30, 42, 44, 58, and 72 amu strongly increase in intensity in the static SIMS spectra of the treated polymer surface. A series of peaks at 74, 90, 102, 118, 130, 149, and 150 amu appear in the spectrum of the plasma-treated polyimide, consistent with chain scission at the C–N bond between the ether and the imide groups. The oxygen content of the surface

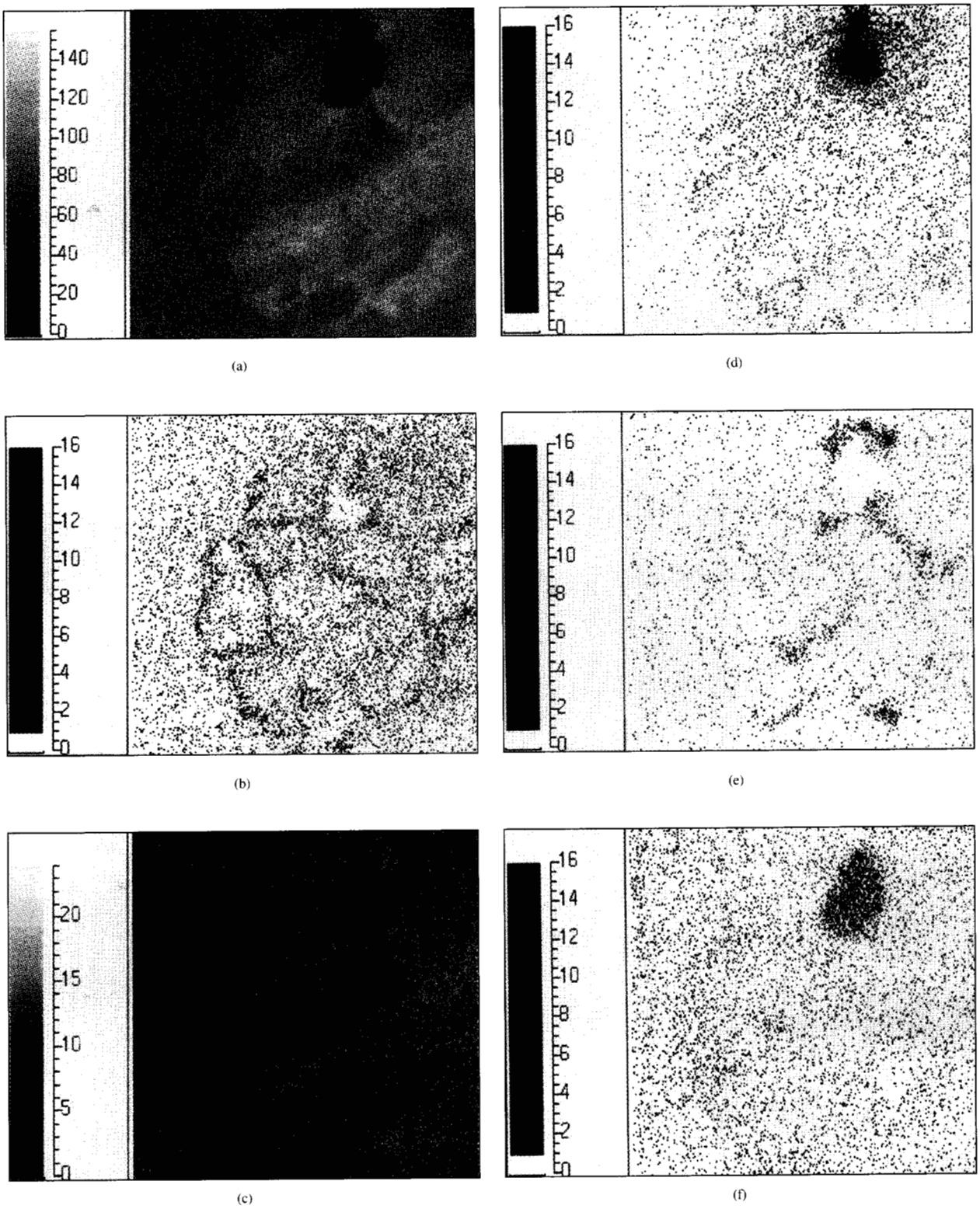

Figure 5

Mass-selected positive ion images of the defect shown in Figure 4 after laser shot. (a) Total positive ion image. (b) Co^+ image. (c) $C_2F_5^+$ image (fluoroether lubricant). (d) Cr^+ image. (e) Ni^+ image. (f) $C_4H_9^+$ image.

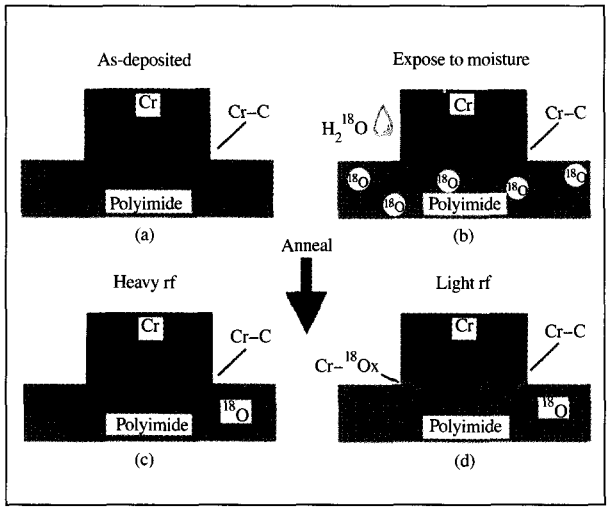

Figure 6

Schematic representation of isotopic water absorption and redistribution after annealing patterned Cr layers deposited onto rf-plasma-treated polyimide. Redrawn from [42], reproduced with permission.

increases either because of the reaction of radicals in the film with trace levels of oxygen in the plasma, or by the reaction of long-lived radicals at the treated surface upon exposure to air.

The adhesion of Cu thin films to polyimide is important for many microelectronic and thin-film packaging applications [40–44]. Both Cr adhesion layers and heat treatments have been used to improve the adhesion between these materials. Preliminary static SIMS measurements suggest that polyimide is chemically altered by deposited metals [40, 41]. Failures of Cu/Cr/polyimide [40, 41] and Cu/polyimide [40] interfaces were induced using peel tests. In all cases, organic material was found on both fracture surfaces. The metals present on each sample were also detected on both fracture surfaces, indicating diffusion of the metals into the polymer. Unsaturation of the polymer was determined using peak ratios of saturated and unsaturated ions such as $C_2H_3^+/C_2H_5^+$ [40]. Higher levels of unsaturation were found on the polymer fracture surface than on unbonded polyimide. This unsaturation was greater when Cr was present and when a heat treatment (300°C, two hours *in vacuo*) was used. The modification of the polymer thus seems to track the improvements in adhesion.

In work related directly to practical microelectronic and thin-film packaging applications, the chromium/polyimide interface has been extensively studied [42–44]. Analyses involving dynamic SIMS, XPS, and AES were performed to determine the mechanism for later degradation of an interface with good initial adhesion. The polyimide surface is altered in the manufacturing environment by sputtering or plasma bombardment cleaning steps. XPS spectra show that graphitization of the polyimide surface is induced by rf Ar plasma bombardment [42]. Auger depth profiles of structures in which the Cr adhesion layer was deposited on rf-modified polyimide show that the carbon at the metal–polymer interface has a "carbidic" peak shape. With thermal cycling, two failure modes are observed. For samples with heavily damaged polyimide, failure occurs within the damaged polyimide just below the Cr/polyimide "carbidic" layer. This near-surface region within the polyimide is oxidized. For samples with lightly damaged polyimide, failure is more catastrophic and involves the formation of chromium oxide at the interface between the "carbidic" layer and the damaged polyimide. Note that failure does not occur at the metal/carbidic carbon interface. The polyimide absorbs water under normal conditions. A key experiment involved the use of ^{18}O-labeled water. The dynamic SIMS profiles showed definitively that this now-labeled absorbed water was the source of oxygen for both failure modes. This result, along with studies of water transport across modified polyimide, led to the hypothesis that the damaged polyimide acts as a barrier to moisture. **Figure 6** is a schematic representation of the redistribution of isotopically labeled water after the annealing step. In samples with an extensive damaged layer (labeled Heavy rf in the figure), migration of water into the Cr-rich carbidic layer is blocked, and failure occurs within this now-^{18}O-labeled damaged layer. In samples which have damaged layers too thin to block water transport (labeled Light rf in the figure), migration of Cr to the carbidic carbon/polyimide interface is followed by formation of an ^{18}O-labeled Cr oxide layer in which catastrophic failure occurs.

Static SIMS spectra of the fracture surfaces from peel-test-failed gold/polytetrafluoroethylene (PTFE) interfaces fail cohesively in the PTFE [39]. Evaporation of gold onto PTFE with simultaneous bombardment by low-energy Ar^+ ions produces an interface with a much improved peel strength that also fails cohesively in the PTFE. Static SIMS data show that the near-interface PTFE layer where cohesive failure occurs is altered by the ion beam bombardment. The ratios of peaks due to high-mass-fragment ions $C_6F_{11}^+$ and $C_7F_{13}^+$ to the CF^+ peak are five times greater in the spectra of the ion-beam-altered interface than in the spectra of the unmodified interface. Similar intensity increases with ion bombardment of PMMA surfaces have been interpreted as being due to chain scission [35] (see above). Chain scission might improve adhesion through strain relief. Alternatively, these results may be interpreted as indicating ion-beam-induced crosslinking [39]. More highly branched fragments have

higher ion yields. Increased crosslinking is expected to improve shear strength.

The interaction of squalene (a model compound) and cis-polyisoprene with steel was studied by static SIMS in conjunction with XPS [45]. The squalene and the polymer react with freshly abraded steel at 160°C. Methyl groups are oxidized to aldehydes and, for the terminal methyl on squalene, to carboxylic acids. The αC–C bonds oxidize to form double bonds, making the polymer at the interface conjugated. C–C crosslinking also increases at this interface. The authors speculate that the conjugated polymer forms π-bonds with the metal surface.

• *Silanes and adhesion*

Silanes are used as adhesion promoters in a variety of situations [46]. Static SIMS studies have not only detected these compounds at surfaces, but have begun to unravel the chemistry that makes them work.

It is a tacit assumption that a covalent bond is formed between silanes and the surfaces to which they promote adhesion. An OH group on the substrate is expected to displace an alkoxy or hydroxy group on the silane to form a Si–O–substrate bond. The most direct evidence for this bonding would be the presence of $FeSiO_x^+$ ions in SIMS spectra of steel surfaces primed with silanes [47–49]. Some question remained as to the true identities of peaks assigned to these ions in early quasistatic spectra of silane-primed steel surfaces [47, 48]. A recent study employs a TOF system with higher mass resolution to unequivocally identify these peaks as belonging to species that do not contain Fe [49]. The correlation that exists between the presence of these ions and the extent to which bonds to these surfaces are weakened by immersion in water [47] may be a measurement of silane coverage. $C_2H_3SiOFe^-$ and $C_3H_{11}NFeO_2^+$ ions that were found in the spectra of steel surfaces treated with 3-aminopropyltrihydroxysilane (3-APTHS) give evidence respectively of metallosiloxane bond formation and interaction of the amine with the surface [49]. Alternatively, these ions may result from etching of the steel surface by the silane solution and may not be indicative of surface-bonding mechanisms.

Indirect proof of covalent attachment was provided by isotopic labeling experiments [50]. **Figure 7** summarizes some potential attachment mechanisms for 3-APTHS to a surface. Figures 7(a) and 7(b) detail the condensation attachment mechanism described above. Subsequent polymerization of the surface-bound silane is expected [Figure 7(c)]. Alternatively, aminosilanes may adsorb non-covalently, as shown in Figures 7(d) and 7(e). An additional non-covalent adsorption mechanism not shown is hydrogen bonding of silanol groups to surface oxides and hydroxides. ^{18}O-labeled 3-APTHS was deposited on Si and Cr surfaces treated with a water plasma. Static SIMS measurements of the resulting surfaces were performed to

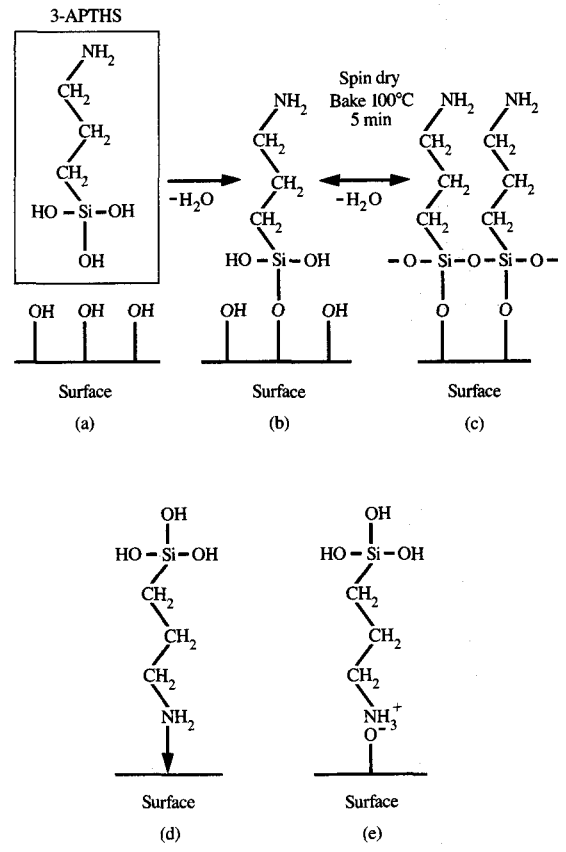

Figure 7

Potential attachment mechanisms for 3-APTHS. (a)–(c) Condensation attachment mechanism. (d) Attachment of molecule via donation of nitrogen lone pair electrons. (e) Attachment of molecule via protonation of amine with surface hydroxyl group. From [50], reproduced with permission.

determine the ^{18}O isotopic enrichment of the surface after reaction with the silane. Possible outcomes of the experiment are shown in **Figure 8**. If the silane is bound covalently to the surface, silane fragments should contain both ^{16}O and ^{18}O [Figure 8(a)]. Silane attachment by non-covalent mechanisms should not reduce the isotopic enrichment of the silane [Figures 8(b) and 8(c)]. The observed ^{16}O:^{18}O ratios for the SiO_2^- ion, which vary from 0.28:0.72 to 0.30:0.70, fall nicely into the expected range for covalent attachment [Figure 8(a)]. Subsequent heating of the surface *in vacuo* (100°C to 120°C for one hour) had little effect on the spectra. In this system, the heating step does not promote further polymerization of the attached silane.

Spectral differences between metal surfaces treated with silanes have been interpreted as reflecting differences in

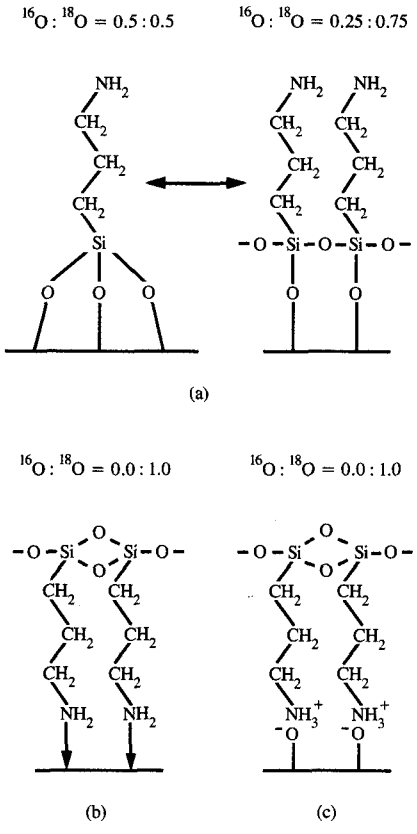

Figure 8

Simple model for predicting the ^{16}O : ^{18}O ratio in observed secondary ions as a function of bonding configuration. (a) Condensation allows for a range of abundances depending on the number of bonds between the silane molecule and the surface. (b), (c) Electron donation and protonation models both predict that no mixing of ^{16}O : ^{18}O should be observed. From [50], reproduced with permission.

silane orientation [49, 51]. The spectra of thin films of N-(2-(vinylbenzylamino)-ethyl)-3-aminopropyltrimethoxy silane (SAAPS) on Zn surfaces have a strong peak due to $C_9H_9^+$, a fragment of the vinylbenzyl group [49]. In thicker films, the intensity of this peak is reduced, while Si-containing peaks gain in intensity. These results suggest that the thin silane films are oriented with the silanol ends close to the Zn substrate and the vinylbenzyl groups close to the surface. Peaks due to N-containing ions have a high intensity in static SIMS spectra of thin films of N-(2-aminoethyl)-3-aminopropyltrimethoxy silane (AEAPS) deposited from solutions at the unadjusted pH of 10.4 onto steel substrates [51]. Lower-pH solutions (8.0) produce films with spectra that have weaker signals due to N-containing ions. The amine ends of the silane are likely oriented toward the steel substrate. Relative to the spectra of AEAPS deposited onto steel, both N- and Si-containing ions are suppressed in spectra of AEAPS films on Zn. Yields of hydrocarbon fragments in the AEAPS/Zn spectra are high. The amphoteric zinc oxide likely interacts with both ends of the silane, leaving only the hydrocarbon middle of the molecule oriented toward the surface.

Additional observations on the interaction of SAAPS with Zn surfaces showed that in thick films the vinyl groups polymerize, that incomplete hydrolysis of the silane can be observed in thin SAAPS films on Zn, and that upon heating the films in air, the silane is partly oxidized [49]. Detection of high-mass ions due to dimers and trimers show that polymerization of the vinyl groups occurs. Large ion fragments of silanes with methoxy groups still attached prove that these molecules have been incompletely hydrolyzed. The appearance of the $C_9H_9O_2^+$ ion in the spectra of the heated films supports the conclusion that the vinylbenzyl groups oxidize.

AEAPS improves the torque/sheer-tested adhesion strength of solution-deposited polystyrene to steel by up to a factor of two [48]. SIMS results show that the silane displaces hydrocarbons as it attaches to the steel surface. Covalent bonding is not possible between the amine groups and the polystyrene. Either entanglement between the silane and polymer chains, and/or interactions between the amine groups of the silane and the polarizable aromatic rings in the polystyrene, are responsible for the improvement in adhesion strength.

Static SIMS analyses have been performed on silane films used to improve the adhesion of paint to steel [52]. Films prepared from solutions of SAAPS and glycidoxypropyltrimethoxy silane (GPS), along with films prepared with mixtures of each of these silanes with the silane crosslinker 1,2-bis(trimethoxysilyl) ethane (TMSE), were analyzed. The crosslinker further improves paint adhesion. While SAAPS films are readily distinguishable from GPS films by SIMS, spectra of SAAPS/TMSE films are nearly identical to spectra of GPS/TMSE films. These spectra are dominated by ion fragments of TMSE. These results suggest that TMSE segregates to the surface of these films. While the other silanes are completely hydrolyzed, methoxy-containing TMSE fragments show that the TMSE is not. It is the wettable surface of the TMSE that presents itself to the paint.

Perhaps the most exciting static SIMS study of the mechanism for adhesion promotion by amino silanes was performed on the E-glass/silane/epoxy system [53–56]. Glass surfaces with 3-APTHS-derived layers give spectra consistent with polymerized silane [53]. Al from the glass is incorporated into the epoxy film. A polydimethylsiloxane (PDMS) contaminant was also shown to be present. Warm water extraction of this surface

reduces the PDMS contamination and reveals an even more highly polymerized epoxy film having spectra with higher-molecular-weight fragments. Spectra of glass slides coated with 3-APTHS and subsequently treated with the epoxy component diglycidyl ether of bisphenol S (DGEBS) contain peaks due to ion fragments of the reaction product of DGEBS with the amino silane [54]. Subsequent work similarly showed the covalent attachment of the diglycidyl ether of bisphenol A (DGEBA) to the amino silane layer [55]. In addition, mass resolved images of both E-glass slides and E-glass fibers demonstrated uniform coverage of the silane. The epoxy resin subsequently coats areas that are not also rich in Al. The question of why some fibers not treated with 3-APTHS had an interfacial sheer strength comparable to that of treated fibers was resolved when static SIMS spectra showed the presence of a 3-APTHS-derived layer on the supposedly untreated surface [56].

Static SIMS detected 3-methacryloxypropyltrimethoxysilane-derived layers on treated E-glass, alumina, and quartz surfaces [57]. Hydrolysis of the silanes appeared to be complete, based on the absence of the OCH_3^+ ion. The presence of peaks due to the $SiOH^-$, SiO_2H^-, and SiO_3H^- ions in the spectra of the E-glass and alumina surfaces provided some evidence for the presence of further unreacted silanol groups (SiOH). No such evidence was found for the quartz surface. The acrylic end of the silane on the quartz surface had polymerized. Peaks attributable to the presence of a polymethacrylate are prominent in the spectrum of the quartz surface, while peaks attributable to individual methacryloxy groups are more prominent in the spectra of the other two treated surfaces. These results suggest greater coverage of the quartz surface, but quantitative XPS work determined that the coverages are comparable on the different surfaces. The apparent presence of more silane–silane bridges (implied by the absence of silanol groups) and of the polymethacrylate suggests closer packing, and consequent island formation on the quartz surface.

At an S-glass/polysulfone joint, ISS and quasistatic-SIMS measurements show that failure is cohesive in the polysulfone [58]. Failure is cohesive even when 3-APTHS is used as an adhesion promoter to double the strength of the bond. While cohesive, these failures take place within 2–3 nm of the S-glass/polysulfone (or silane/polysulfone, when 3-APTHS was used) interface. Fluorine and alkali metal concentrations are elevated at the fracture surfaces. This result indicates that the near-interface polysulfone layer is altered by diffusion of impurities from the glass surface.

3-aminopropyltrimethoxysilane is mixed with silicone RTV and used as an adhesion promoter for the metal/RTV elastomer interface. Dynamic SIMS depth profiles showed, using a deuterated silane, that this promoter is uniformly distributed in the elastomer and does not segregate to the interface [59]. The result opens the possibility that the promoter acts by altering the bulk properties of the RTV elastomer rather than by increasing the strength of the interface.

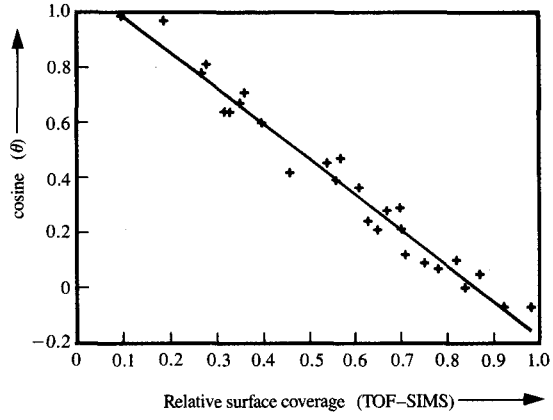

Figure 9

Relative surface coverage for trimethylsilylated silicon wafers, as measured by TOF–SIMS, plotted as a function of the cosine of the contact angle. The line drawn corresponds to the following equation, calculated by the method of least squares for all data points: $\cos\theta = -1.30f + 1.12$, where f is the surface coverage by the TMS groups. From [60], reproduced with permission.

Hexamethyldisilazane (HMDS) and trimethylsilyldiethylamine (TMSDEA) are typically used in the semiconductor industry as "adhesion promoters" for photoresist on silicon wafers. The attachment of trimethylsiloxyl (TMS) groups on silicon wafers actually reduces the initial adhesion of the photoresist to the silicon surface [60]. The hydrophobic TMS groups prevent penetration of the developer solution, used to remove exposed photoresist, to the interface between unexposed resist and the wafer. Lift-off is thus prevented, and the TMS is properly called an adhesion promoter under these circumstances. Static SIMS was used in conjunction with contact angle measurements to quantitatively measure the surface coverage of TMS on silicon. This surface coverage was, in turn, correlated with lift-off. A plot of the ratio of the $(CH_3)_3Si^+$ and Si^+ peak intensities against the cosine of the contact angle is linear (**Figure 9**). This indicates that the surface coverage is directly proportional to the SIMS intensity ratio. With the assumption that the maximum intensity measured for any sample is one monolayer, the percentage monolayer coverage was determined directly from SIMS data. Unlike contact angle data, the SIMS data were relatively insensitive to the presence of other adsorbates (contaminants) on these

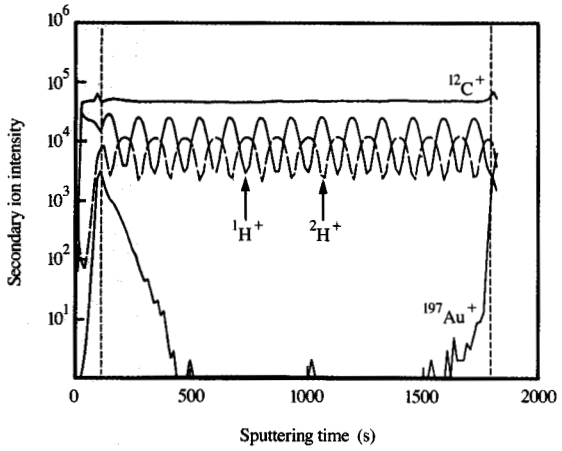

Figure 10

SIMS depth profile of $^1H^+$, $^2H^+$, $^{12}C^+$, and $^{197}Au^+$ obtained from a 500-nm-thick film of PSD/PMMA which was heat-treated at 170°C for 72 hours. From [63], reproduced with permission.

wafers. It was concluded using the SIMS data that at least 50% monolayer coverage of TMS was needed to prevent developer-induced lift-off.

- *Polymer interfaces*

The applications of SIMS to solving problems in polymer science have increased in recent years. Those applications that have relevance to the problem of adhesion are reviewed here [61–71]. Although significant organic fragments are lost from the spectrum after any significant sputtering, isotopic labeling allows depth profiling by dynamic SIMS of particular polymer elements. Dynamic SIMS has greater depth resolution than forward recoil elastic scattering (FRES), and the data it provides are more readily interpretable than neutron reflectivity (NR) data [61, 62]. Static SIMS has proven particularly useful in the detection of polymer additives [29, 59]. Static SIMS has also been applied to the characterization of epoxy adhesives [70, 71] and polyethylene/epoxy joints [7].

A series of experiments were performed on the behavior of symmetric diblock copolymers alone and in conjunction with other polymer layers [63–66]. These copolymers consisted of a block of polystyrene (PS) joined to a block of polymethylmethacrylate (PMMA). One or both of the blocks were perdeuterated.

In a study of layers of these copolymers with perdeuterated polystyrene blocks [63], the polymers were spun-cast onto silicon wafers or silicon wafers coated with gold. Initial depth profiles of these films showed an even distribution of carbon, hydrogen, and deuterium, indicating random orientation of the polymer in the film. Treatment of the film by heating it above its glass transition temperature orders the polymer chains perpendicular to the substrate surface. The ordering of the polymer chains segregates the PS and PMMA segments of the copolymer into discrete layers. This was demonstrated by the oscillations of hydrogen and deuterium intensities apparent in the SIMS depth profiles (**Figure 10**). Polystyrene preferentially segregates to the low-energy air and nonpolar gold surfaces, while the more polar PMMA end of the copolymer segregates to the native oxide at the silicon surface. The segregation of this polymer to attain the lowest-energy interface has obvious consequences for the processing of polymers to enhance adhesion.

In a related experiment, both blocks of this copolymer were perdeuterated and mixed with homopolymeric polystyrene [64]. As cast, the copolymer segregates to the oxidized silicon interface because of the affinity of the PMMA for the oxide. After heating of the film to the glass transition temperature, further segregation of the copolymer to both the substrate and air interfaces was clear from the SIMS depth profiles. The immiscibility of the PMMA chain in the polystyrene provides the thermodynamic driving force for segregation. The implication for adhesion of polymer films is clear. The PMMA segregates to the less favored air interface as a result of its poor interaction with the bulk of the polymer film.

The adhesion of two immiscible polymer layers can be enhanced by the addition of a diblock copolymer to the interface [65, 66]. This was demonstrated with homopolymer layers of PMMA and poly(2,6-dimethyl-1,4-phenylene oxide) (PPO). By perdeuterating one of the PMMA–PS copolymer blocks and using dynamic SIMS, the copolymer was shown to orient itself along the interface with the PMMA block of the copolymer on the PMMA side of the interface and the PS block on the PPO side [65]. For copolymer thicknesses of less than $L/2$ (where L is the long period of the pure copolymer), fracture failure occurs at the covalent link between the two copolymer blocks, centered at the PMMA/PPO interface [66]. The addition of the copolymer to this interface improves the interface fracture toughness by as much as two orders of magnitude. Creton et al. tracked the fracture toughness and the exact location of failure as determined by SIMS as a function of copolymer thickness at the interface [66]. These measurements demonstrated the effectiveness of polymer chain entanglement in promoting adhesion.

By combining isotopic labeling with dynamic SIMS, strong support has been garnered for the reptation theory of polymer diffusion in a melt [67]. This theory describes

a polymer motion in which a snake-like chain moves in the direction of its length through tubes defined by entanglements surrounding the chain. Two PS layers were joined: one labeled with deuterium at the chain ends and the other with deuterium in its middle. As the glass transition temperature is reached, the polymers diffuse into each other. If the chains move along their length, at some point only the ends of the chains will have crossed the interface. One side of the interface will then be rich in deuterium and the other rich in hydrogen. This ripple effect was clearly observed in dynamic SIMS depth profiles (**Figure 11**).

While deuterium is often treated as being identical to hydrogen, a small difference in the polarizability of the C–D bond exists relative to the C–H bond. For the studies described above, this small difference is not significant when compared to the larger thermodynamic effects of having chemically different polymer segments. But where a homopolymer is partially perdeuterated, this difference is sufficient to cause some segregation [68, 69]. Dynamic SIMS profiles of a mixture of PS and perdeuterated PS clearly showed segregation of the perdeuterated polymer to the air interface. The exact shape of the depth profile was modeled by a theory intended to predict polymer segregation [69]. Segregation of this kind works to improve the adhesion strength of a polymer to a second phase, and that segregation is facile even when the thermodynamic driving force is small.

For a non-isotopically labeled polymer joint, dynamic SIMS is not sufficient to characterize the failed interface. Examples of a polymer joint where the two polymers are readily distinguishable by static SIMS is the low-density polyethylene (LDPE) or high-density polyethylene (HDPE)/epoxy bond [7]. For the HDPE/epoxy interface, failure was clearly interfacial. For the LDPE/epoxy interface, some hydrocarbon transfer to the epoxy adhesive surface was detected, but the strong negative ion spectrum characteristic of the adhesive showed that the LDPE transfer to the adhesive was patchy. XPS results confirmed that material transfer was submonolayer. The transfer may be due to mobile low-molecular-weight or less-crystalline material in the LDPE.

Static SIMS spectra of epoxy adhesives can be readily interpreted in terms of fragments of epoxide structures [70, 71]. The ratio of bisphenol A to terminal epoxide components increases with increasing molecular weight. This is accompanied by an increase in the ratio of the characteristic fragments for these species in the SIMS spectra [71]. On the basis of this work, determination of the concentration of epoxide end groups at a surface by static SIMS should be possible.

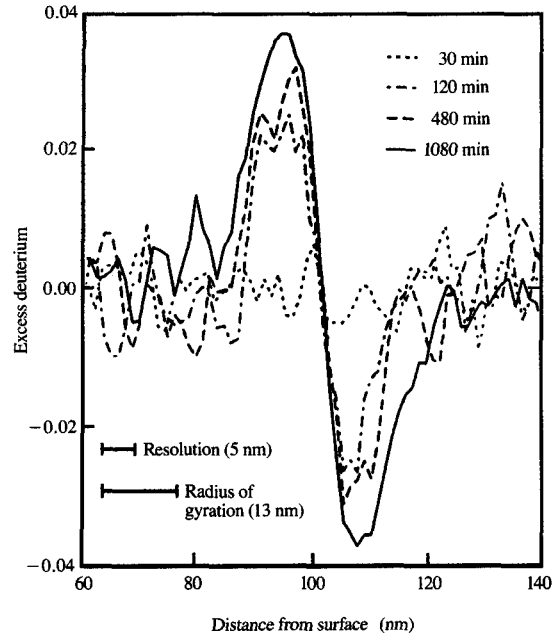

Figure 11

Excess deuterium determined by dynamic SIMS as a function of distance for the HDH and DHD polystyrene bilayers after interdiffusion at 112°C for the times specified. In all cases the amplitude of the excess deuterium is increasing with time. From [67], reproduced with permission.

• *Interface width measurements*

As with other depth profiling techniques, dynamic SIMS can determine the width of a sufficiently broad interface and can detect diffusion across an interface [72–81]. The advantage of dynamic SIMS is its sensitivity.

Dynamic SIMS analysis of Ag layers deposited onto glass through decomposition of organometallic resinate solutions indicates that glass components (Fe, B, alkali metals) diffuse into the deposited layer [72]. SIMS is profoundly sensitive to the alkali metals and far more sensitive to Fe and B than is AES or XPS. The authors suggest that oxygen depletion of the glass side of the interface (detected by XPS and ISS) which accompanies the diffusion of other glass components into the Ag layer allows the formation of Ag–Si bonds. This hypothesis is supported by previous examples of Ag–Si bonding, and provides an explanation for the strength of this interface. An additional observation of fluctuations of the Ag ion intensity in the SIMS depth profile can be explained by the presence of hydrocarbons trapped in voids in the Ag layer. As the Ag ion intensity decreases, the intensity of peaks ascribed to hydrocarbons increases.

Cu films were deposited on cordierite-type ceramics by plasma-aided physical vapor deposition (ion-plating) [73]. Adhesion tests that involve pulling on an epoxy-bonded stud to produce failure show an increase in adhesion strength for films produced at higher bias voltages. The dynamic SIMS depth profiles show that a gradient of Al, Mg, and Si from the ceramic extends far into a well-adhered Cu film. Ion-beam-enhanced mixing in the ion-plating process is the likely cause for the gradients and the adhesion improvements.

Ion beam mixing has been intentionally used to improve adhesion [74–76]. Ion beam mixing of the $TiN/W_{18}Cr_4V$ (high-speed steel) interface was responsible for greatly improved adhesion strength [74]. The scratch-test-measured critical load is proportional to the dynamic SIMS measured width of the mixed interface. Adhesion of sputtered MoS_x lubricating films to steel was also enhanced by ion beam mixing [75, 76]. Dynamic SIMS showed that mixing of the MoS_x/substrate interface accompanied the enhanced sliding life of these films.

The effects of reactive and nonreactive ion beam mixing on Ni and Ti films deposited on various carbon substrates have been studied [77, 78] using dynamic SIMS, AES, XPS, scanning electron microscopy with energy-dispersive X-ray analysis (SEM with EDX), and X-ray diffraction (XRD). Scratch tests were employed to measure the adhesion. Dynamic SIMS and AES were used to determine the extent of interfacial mixing and diffusion of the metals into the carbon substrates. Dynamic SIMS profiles of the Ni films showed little interfacial mixing or diffusion [77]. Significant topological changes were observed by SEM and TEM after ion implantation. These results indicate that Ni adhesion improvements by ion implantation are the result of mechanical interlocking of the Ni films with the carbon substrates. Mixing is suppressed because the formation of Ni carbide is thermodynamically unfavorable. In contrast, Ti carbide forms quite readily, and dynamic SIMS profiles showed substantial mixing at the Ti–carbon interface [78]. XPS confirmed that carbide formation had taken place at the interface. Adhesion increases with ion implantation were quite large for most samples. Implantation of 5×10^{16} Kr/cm^2 at 400°C, however, did not improve the adhesion of a Ti film deposited on a-face pyrolytic graphite. Dynamic SIMS detected a discrete oxide layer at the interface of this sample. The oxide probably prevented carbide formation and acted as a weak boundary layer which caused adhesion loss.

Dynamic SIMS profiles cannot be used to distinguish between interdiffusion and mechanical interlocking as mechanisms for adhesion improvement. An example of this problem can be found in the study of the surface preparation of Ni and Inconel substrates by ion beam sputtering [79]. Sputtering for a short time produces a dramatic increase in the scratch-tested adhesion of deposited Cu layers to these substrates. This is probably due to removal of a weak surface layer produced during mechanical polishing. Longer sputter times further enhance adhesion. Dynamic SIMS profiles show that the interface between deposited Cu layers and these substrates broadens with increasing ion bombardment times. SEM photographs show that increased ion bombardment induces continued surface roughening. These results suggest that the adhesion improvements are due to increased mechanical interlocking.

After bombardment with a MeV ion beam to enhance adhesion, dynamic SIMS was used to look for interdiffusion at the interface [80, 81]. While Rutherford backscattering (RBS) was used to measure the mixing in MeV ion implanted films in the Ag/Ta and Ag/Ta_2O_5 systems, Ag atom migration was only detected when SIMS and AES were used [81]. The sensitivity of RBS was not sufficient to detect the low levels of Ag diffusion found for these samples.

Summary

The SIMS experiment is simple conceptually. Primary ions strike the sample, generating secondary ions which are detected by a mass spectrometer. A brief description of SIMS and of how SIMS analyses are performed has been presented.

The SIMS technique has made a significant impact on the study of adhesion. SIMS measurements have been used to explore the nature of surfaces prepared for bonding. The sensitivity of this technique has been applied to the analysis of contaminants that produce interfacial failures. The molecular specificity of SIMS has been used to determine how polymers are damaged by cleaning and deposition techniques. The mechanism of adhesion promotion by silanes has been extensively studied using SIMS. Polymer/polymer interfaces have been characterized with SIMS depth profiles. Depth profiles have also been used to measure interface widths.

The understanding of how to fully exploit SIMS is improving rapidly; the pace of the work on the application of SIMS to the study of adhesion is accelerating. It is hoped that this summary of the literature to date will provide a basis for the continued growth of this field.

Acknowledgments

The author would like to thank D. Pocker and B. Prime for valuable suggestions and discussions, and J. Parker for his help in depicting the sputter event.

References

1. W. C. Wake, *Adhesion and the Formulation of Adhesives*, 2nd Edition, Applied Science Publishers LTD, London, 1982.

2. Allen R. Madura, "ISS/SIMS Can Help You Understand Your Bonding Failures," *Ind. Res. Develop.*, pp. 98–101 (August 1982).
3. Gene R. Sparrow, "Characterization of Cleaned and Bonding Surfaces by ISS/SIMS," *Manuf. Eng. Trans.* **6**, 1–10 (1978).
4. W. L. Baun, "Applications of Surface Analysis Techniques to Studies of Adhesion," *Appl. Surf. Sci.* **4**, 291–306 (1980).
5. W. L. Baun, "Use of Secondary Ion Mass Spectrometry to Study Surface Chemistry of Adhesive Binding Materials," *Desorption Mass Spectrometry, Are SIMS and FAB the Same?*, Philip A. Lyon, Ed., *ACS Symp. Ser.* **291**, 227–241 (1985).
6. D. Briggs, "New Developments in Polymer Surface Analysis," *Polymer* **25**, 1379–1391 (1984).
7. D. Briggs, "Application of Secondary Ion Mass Spectrometry to Adhesion Studies," *J. Adhesion* **21**, 343–352 (1987).
8. Joseph A. Gardella, Jr., "Principles and Applications of Photoelectron and Ion Spectroscopy for the Analysis of Polymer Surfaces," *Analysis of Paints and Related Materials: Current Techniques for Solving Coatings Problems*, ASTM, Philadelphia, 1992, pp. 157–170 [ASTM Special Technical Publication 1119, 157–170 (1992)].
9. Wayne Niemeyer and John Gavrilovic, "What's Wrong with the Surface?" *Research & Development* **27**, 114–117 (1985).
10. P. Sigmund, "Sputtering by Ion Bombardment: Theoretical Concepts," *Sputtering by Particle Bombardment I*, R. Behrisch, Ed., Springer-Verlag, Berlin, 1981, pp. 9–69.
11. A. Benninghoven, F. G. Rudenauer, and H. W. Werner, *Secondary Ion Mass Spectrometry: Basic Concepts, Instrumental Aspects, Applications and Trends*, John Wiley & Sons, Inc., New York, 1987.
12. *Secondary Ion Mass Spectrometry Principles and Applications*, John C. Vickerman, Alan Brown, and Nicola Reed, Eds., Clarendon Press, Oxford, U.K., 1989.
13. *Practical Surface Analysis*, 2nd Edition, Vol. 2, *Ion and Neutral Spectroscopy*, D. Briggs and M. P. Seah, Eds., John Wiley, New York, 1992.
14. D. F. Reich and B. W. Schueler, "Depth Profiling Capabilities Offered by Time-of-Flight SIMS: Recent Developments," *Proceedings of the Ninth International Conference on Secondary Ion Mass Spectrometry (SIMS IX)*, Yokohama, Japan, November 8–12, 1993 (John Wiley, New York, 1994).
15. F. Bouquet, J. M. Cuntz, and C. Coddet, "Influence of Surface Treatment on the Durability of Stainless Steel Sheets Bonded with Epoxy," *J. Adhesion Sci. Technol.* **6**, 233–242 (1992).
16. Markus Amstutz and Marcus Textor, "Applications of Surface Analytical Techniques to Aluminium Surface in Commercial Semifabricated and Finished Products," *Surf. Interface Anal.* **19**, 595–600 (1992).
17. P. L. J. Gunter, H. J. Borg, J. W. Niemantsverdriet, and H. J. H. Rheiter, "Take-Off Angle Dependent X-ray Photoelectron Spectroscopy, Secondary Ion Mass Spectrometry, and Scanning Electron Microscopy for Determining the Thickness and Composition of Passivation Layers on Technical Aluminum Foils," *J. Vac. Sci. Technol. A* **10**, 2846–2851 (1992).
18. W. L. Baun, "The Effect of Etching on Ti_6Al_4V Interfacial Chemistry and Adhesion to Evaporated Gold and a Commercial Adhesive," *J. Adhesion* **12**, 81–98 (1981).
19. Ronald S. Nowicki, Patrice Geraghty, David Harris, Gayle Lux, and David J. Johnson, "In Situ Native Oxide Clean Followed by Chemical Vapor Deposition of Tungsten Silicide on Polysilicon in a Cluster Tool," *J. Vac. Sci. Technol. A* **9**, 1073–1082 (1991).
20. P. Phuku, P. Bertrand, and Y. de Puydt, "Adhesion, Microstructure and Composition of Thermally Evaporated Aluminum Thin Layers on Polyethylene Terephthalate Films," *Thin Solid Films* **200**, 263–274 (1991).
21. H. Haidara, Y. Papirer, M. F. Vallat, and J. Schultz, "Relationship Between Structural Properties of Vapour-Deposited Metallic Films on to Polymer and Their Relative Adhesive Performance," *J. Mater. Sci.* **28**, 3243–3246 (1993).
22. Y. de Puydt, P. Bertrand, and P. Lutgen, "Study of the Al/PET Interface in Relation with Adhesion," *Surf. Interface Anal.* **12**, 486–490 (1988).
23. J. Lub, P. N. T. van Velzen, D. van Leyen, B. Hagenhoff, and A. Benninghoven, "TOF-SIMS Analysis of the Surface of Insulators. Examples of Chemically Modified Polymers and Glass," *Surf. Interface Anal.* **12**, 53–57 (1988).
24. J. W. Severin, R. Hokke, H. van der Well, and G. de With, "A Study on Changes in Surface Chemistry During the Initial Stages of Electroless Ni(P) Deposition on Alumina," *J. Electrochem. Soc.* **140**, 682–687 (1993).
25. J. W. Severin, R. Hokke, and G. de With, "Adhesion of Electrolessly Deposited Ni(P) Layers on Alumina Ceramic. I. Mechanical Properties," *J. Appl. Phys.* **75**, 3402–3413 (1994).
26. J. W. Severin, R. Hokke, H. van der Wel, and G. de With, "Adhesion of Electrolessly Deposited Ni(P) Layers on Alumina Ceramic. II. Interface Characterization," *J. Appl. Phys.* **75**, 3414–3422 (1994).
27. W. L. Baun, "Use of Ion Scattering and Secondary Ion Mass Spectrometry to Characterize Apparent Adhesive Failure in an Adhesive Bond," *J. Adhesion* **7**, 261–267 (1976).
28. J. E. de Vries, T. L. Riley, J. W. Holubka, and R. A. Dickie, "Surface Studies of Conversion Coated Steel After Corrosion Induced Paint De-Adhesion" *Surf. Interface Anal.* **7**, 111–116 (1985).
29. Judith Stein, Tracey M. Leonard, and Gary Smith, "Application of the Dynamic-SIMS Technique to the Study of Silicone Release Coatings," *J. Appl. Polym. Sci.* **42**, 2355–2360 (1991).
30. A. J. Paul and J. C. Vickerman, "Organics at Surfaces, Their Detection and Analysis by Static Secondary Ion Mass Spectrometry," *Phil. Trans. Roy. Soc. Lond. A* **333**, 147–158 (1990).
31. Jane Gates Jinkins, Richard Kvitek, Guillermo Prada-Silva, and Alan Brown, "Use of TOF-SIMS and XPS to Characterize Surfaces of Thin Metal Films for Evaluation of Bondability," presented at the 40th National American Vacuum Symposium, Orlando, FL, November 15–19, 1993.
32. C. L. Zhao, F. Dobler, T. Pith, Y. Holl, and M. Lambla, "Surface Composition of Coalesced Acrylic Latex Films Studied by XPS and SIMS," *J. Colloid Interface Sci.* **128**, 437–449 (1989).
33. *Laser Ionization Mass Analysis*, Akos Vertes, Renaat Gijbels, and Fred Adams, Eds., John Wiley, New York, 1993.
34. S. Waddington and D. Briggs, "Adhesion Mechanisms Between Polymer Coatings and Polypropylene Studied by XPS and SIMS," *Polymer Commun.* **32**, 506–508 (1991).
35. D. Briggs and M. J. Hearn, "Interaction of Ion Beams with Polymers, with Particular Reference to SIMS," *Vacuum* **36**, 1005–1010 (1986).
36. H. van der Wel and J. Lub, "Surface Modification of Polymethylmethacrylate by UV Light as Studied by TOF-SIMS," *Surf. Interface Anal.* **20**, 373–378 (1993).
37. J. Lub, F. C. B. M. van Vroonhoven, and A. Benninghoven, "The Interaction of Hydrogen and Ammonia Plasmas with Polymethacrylic Esters, Studied

by Static Secondary Ions Mass Spectrometry," *J. Polymer Sci.: Part A: Polymer Chem.* **27**, 4035–4049 (1985).
38. E. Niehuis, P. N. T. van Velzen, J. Lub, T. Heller, and A. Benninghoven, "High Mass Resolution Time-of-Flight Secondary Ion Mass Spectrometry: Application to Peak Assignments," *Surf. Interface Anal.* **14**, 135–142 (1989).
39. W. J. van Ooij, "Characterization of Interfaces Between Polymers and Metals by Static-SIMS," *Electronic Packaging Materials Science IV Symposium Proceedings*, R. Jaccodine, Ed., 1989 [*MRS Symp. Proc.* **153**, 149–155 (1989)].
40. W. J. van Ooij, R. H. G. Brinkhuis, and J. M. Park, "Adhesion of Copper and Chromium Films to Polyimide Studied by Static-SIMS of the Interface," *Surf. Interface Anal.* **12**, 505–506 (1988).
41. C. H. Yang and P. C. Chen, "The Aspects of Thermal Anneal to Intrinsic Stress and Microstructure of Multilayer Thin Films," *Electronic Packaging Materials Science IV Symposium Proceedings*, R. Jaccodine, Ed., 1989 [*MRS Symp. Proc.* **154**, 335–342 (1989)].
42. B. K. Furman, K. D. Childs, H. Clearfield, R. Davis, and S. Purushothman, "Moisture Induced Interfacial Oxidation of Chromium on Polyimide," *J. Vac. Sci. Technol. A* **10**, 2913–2920 (1992).
43. K. Seshan, S. N. S. Reddy, and S. K. Ray, "Adhesion of Thin Metal Films to Polyimide," *1987 Proceedings of the 37th Electronic Components Conference*, Boston, May 11–13, IEEE, New York, 1987, pp. 604–608.
44. B. K. Furman, S. Purushothaman, E. Castellani, and S. Renick, "Mechanical and Surface Analytical Studies of Titanium/Polyimide Adhesion," *Proceedings of the Symposium on Multilevel Metallization, Interconnection, and Contact Technologies*, IEEE, New York, 1987, pp. 142–151.
45. W. J. van Ooij and V. Rangarajan, "Mechanism of Adhesion Between Polyolefins and Steel as Studied by XPS and Static-SIMS," *MRS Symp. Proc.* **119**, 241–246 (1988).
46. *Silanes and Other Coupling Agents*, K. L. Mittal, Ed., VSP, Zeist, The Netherlands, 1992.
47. M. Gettings and A. J. Kinloch, "Surface Analysis of Polysiloxane/Metal Oxide Interfaces," *J. Mater. Sci.* **12**, 2511–2518 (1977).
48. R. A. Cayless and D. L. Perry, "Adhesion Promotion by Silanes: A Study of Their Interfacial Chemistry in a Model Polystyrene Coating by XPS and SIMS," *J. Adhesion* **26**, 113–130 (1988).
49. W. J. van Ooij and A. Sabata, "Characterization of Films of Organofunctional Silanes by TOFSIMS and XPS. Part I. Films of N-(2-(vinylbenzylamino)-ethyl)-3-aminopropyltrimethoxysilane on Zinc and γ-aminopropyltriethoxysilane on Steel Substrates," *J. Adhesion Sci. Technol.* **5**, 843–863 (1991).
50. B. N. Eldridge, L. P. Buchwalter, C. A. Chess, M. J. Goldberg, R. D. Goldblatt, and F. P. Novak, "A Time-of-Flight Static Secondary Ion Mass Spectrometry and X-Ray Photoelectron Spectroscopy Study of 3-aminopropyltrihydroxysilane on Water Plasma Treated Chromium and Silicon Surfaces," *J. Adhesion Sci. Technol.* **6**, 109–125 (1992).
51. W. J. van Ooij and A. Sabata, "Characterization of Films of Organofunctional Silanes by TOF-SIMS. Part II. Films of γ-APS, AEAPS, and FPS on Cold Rolled Steel and Cold Rolled Zinc Substrates," *Surf. Interface Anal.* **20**, 475–484 (1993).
52. Wim J. van Ooij and Ashok Sabata, "Modification of the Interface Between Paints and Stainless Steels by Means of an Interphase of Crosslinked Organofunctional Silanes," *MRS Symp. Proc.* **304**, 155–160 (1993).
53. D. Wang, F. R. Jones, and P. Denison, "TOF SIMS and XPS Study of the Interaction of Hydrolised γ-aminopropyltriethoxysilane with E-Glass Surfaces," *J. Adhesion Sci. Technol.* **6**, 79–98 (1992).
54. D. Wang and F. R. Jones, "ToF-SIMS and XPS Study of the Interaction of Silanized E-Glass with Epoxy Resin," *J. Mater. Sci.* **28**, 1396–1408 (1993).
55. D. Wang and F. R. Jones, "ToF-SIMS and XPS Studies of the Interaction of Silanes and Matrix Resins with Glass Surfaces," *Surf. Interface Anal.* **20**, 457–467 (1993).
56. D. Wang and F. R. Jones, "TOF SIMS and XPS Study of the Interaction of Aminosilanised E-Glass Fibres with Epoxy Resins. Part I: Diglycidyl Ether of Bisphenol S," *Compos. Sci. Technol.* **50**, 215–228 (1994).
57. F. Garbassi, E. Occhiello, C. Bastioli, and G. Romano, "A Quantitative and Qualitative Assessment of the Bonding of 3-methacryloxypropyltrimethoxysilane to Filler Surfaces Using XPS and SSIMS(FABMS) Techniques," *J. Colloid Interface Sci.* **117**, 258–270 (1987).
58. Anthony T. DiBenedetto and Daniel A. Scola, "Characterization of S-Glass/Polysulfone Adhesive Failure Using Ion Scattering Spectroscopy and Secondary Ion Mass Spectrometry," *J. Colloid Interface Sci.* **74**, 150–162 (1980).
59. J. Stein, S. J. Valenty, G. A. Smith, D. V. Brezniak, and L. C. Prutzman, "Location of the Adhesion Promoter (γ-Aminopropyl)trimethoxysilane in a Cured Silicone RTV Matrix," *Macromolecules* **19**, 2291–2294 (1986).
60. J. J. Ponjee, V. B. Marriott, M. C. B. A. Michielsen, F. J. Townslayer, P. N. T. van Velzen, and H. van der Wel, "The Relation Between Lift-Off of Photoresist and the Surface Coverage of Trimethylsiloxy Groups on Silicon Wafers: A Quantitative Time-of-Flight Secondary Ion Mass Spectrometry and Contact Angle Study," *J. Vac. Sci. Technol. B* **8**, 463–466 (1990).
61. T. P. Russell, "The Characterization of Polymer Interfaces," *Annu. Rev. Mater. Sci.* **21**, 249–268 (1991).
62. S. A. Schwarz, B. J. Williams, M. A. A. Pudensi, M. H. Rafaiovich, J. Sokolov, X. Zhao, W. Zhao, X. Zheng, T. P. Russell, and R. A. L. Jones, "Studies of Surface and Interface Segregation in Polymer Blends by Secondary Ion Mass Spectrometry," *Molec. Phys.* **76**, 937–950 (1992).
63. V. R. Deline, G. Coulon, T. P. Russell, and D. C. Miller, "SIMS and Copolymer Ordering," *Secondary Ion Mass Spectrometry—SIMS VII Proceedings of the 7th International Conference*, Monterey, CA, John Wiley, New York, 1989, pp. 359–362.
64. V. S. Wakharta, V. R. Deline, and T. P. Russell, "Depth Profiles of Mixtures of Homopolymers with Symmetric Diblock Copolymers," *ibid.*, pp. 363–366.
65. V. R. Deline, H. R. Brown, and K. Char, "The Use of Secondary Ion Mass Spectrometry to Investigate Copolymer Enhanced Adhesion Between Immiscible Polymers," *J. Vac. Sci. Technol. A* **9**, 1283–1288 (1991).
66. C. Creton, H. R. Brown, and V. R. Deline, "Influence of Chain Entanglement on the Failure Modes in Block Copolymer Toughened Interfaces," *Macromolecules* **27**, 1774–1780 (1993).
67. T. P. Russell, V. R. Deline, W. D. Dozier, G. P. Felcher, G. Agrawal, R. P. Wool, and J. W. Mays, "A Direct Observation of Reptation at Polymer Interfaces," *Nature* **365**, 235–237 (1993).
68. S. A. Schwarz, R. A. L. Jones, E. J. Kramer, M. H. Rafailovich, and J. C. Sokolov, "SIMS Depth Profiling Study of Surface Enrichment in Blends of Deuterated and Protonated Polystyrene," *Secondary Ion Mass Spectrometry—SIMS VII Proceedings of the 7th International Conference*, Monterey, CA, John Wiley, New York, 1989, pp. 355–358.
69. R. A. L. Jones, E. J. Kramer, M. H. Rafailovich, J. Sokolov, and S. A. Schwarz, "Surface Enrichment in Polymer Blends: Simple Theory and an Experimental Test," *Electronic Packaging Materials Science IV*

Symposium Proceedings, R. Jaccodine, Ed., 1989 [*Mater. Res. Soc. Symp. Proc.* **154**, 217–225 (1989)].
70. J. A. Treverton, A. J. Paul, and D. Johnson, "The Application of Static Secondary Ion Mass Spectrometry to the Study of Epoxy Adhesive Constituents," *Intl. J. Adhesion Adhesives* **11**, 158–162 (1991).
71. J. A. Treverton, A. J. Paul, and J. C. Vickerman, "Characterization of Adhesive and Coating Constituents by Time of Flight Secondary Ion Mass Spectrometry (ToF–SIMS) Part I: Epoxy-Terminated Diglycidyl Polyethers of Bisphenol A and Propan-2-ol," *Surf. Interface Anal.* **20**, 449–456 (1993).
72. J. R. Pitts, T. M. Thomas, and A. W. Czanderana, "Surface Analysis of Silver Mirrors Made from Organometallic Solutions," *Solar Energy Mater.* **11**, 261–271 (1984).
73. J. M. Rigsbee, P. A. Scott, R. K. Knope, C. P. Ju, and V. F. Hock, "Structure, Chemistry and Adhesion of Ion-Plated Metal/Ceramic Interfaces," *Fifth International Conference on Ion and Plasma Assisted Technology, IPAT 85*, 1985, pp. 206–211.
74. L. Xiang, T. C. Ma, and Y. C. Zhu, "Stitching TiN Films on High Speed Steel Substrates by Ion Beams," *Mater. Sci. Eng. A* **139**, 193–198 (1991).
75. K. Kobs, H. Dimigen, H. Hubsch, and H. J. Tolle, "Improved Adhesion of Solid Lubricating Films with Ion Beam Mixing," *Philips Tech. Rev.* **44**, 24–29 (1989).
76. K. Kobs, H. Dimigen, H. Hubsch, H. J. Tolle, R. Leutenecker, and H. Ryssel, "Improved Tribological Properties of Sputtered MoS_x Films by Ion Beam Mixing," *Appl. Phys. Lett.* **49**, 496–498 (1986).
77. A. A. Galuska, J. C. Uht, and P. M. Adams, "Reactive and Non-Reactive Ion Mixing of Ni Films on Carbon Substrates," *J. Vac. Sci. Technol. A* **6**, 99–109 (1988).
78. A. A. Galuska, J. C. Uht, and N. Marquez, "Reactive and Non-Reactive Ion Mixing of Ti Films on Carbon Substrates," *J. Vac. Sci. Technol. A* **6**, 110–122 (1988).
79. M. Cahoreau, G. H. Lee, J. Caisso, and M. Cailler, "Adhesion Enhancement of Magnetron-Sputtered Copper Films by Ion Bombardment Etching Treatment of Nickel and Inconel Substrates: Investigations by Auger Electron Spectroscopy and Secondary Ion Mass Spectroscopy of the Ion Beam Effects," *J. Adhesion Sci. Technol.* **5**, 987–999 (1991).
80. B. Daudin and P. Martin, "MeV Ion Beam Enhanced Adhesion of Au Films on Alumina," *Nucl. Instrum. Meth. B* **34**, 181–187 (1988).
81. Yuanxun Qiu, Jiayong Tang, Liqing Pan, Guoqing Zhao, Zhuying Zhou, Xiliang Gu, and Ye Feng, "Interface Adhesion Enhanced by MeV Ions," *Nucl. Instrum. Meth. B* **56/57**, 634–638 (1991).

Received November 5, 1993; accepted for publication September 5, 1994

Alan M. Spool *IBM Storage Systems Division, San Jose facility, 5600 Cottle Road, San Jose, California 95193 (SPOOL at SJEVM13, aspool@vnet.ibm.com).* Dr. Spool is an Advisory Engineer in the IBM Analytical Laboratories at the San Jose Materials Laboratory. He has current responsibilities for all TOF–SIMS work produced in IBM west of the Mississippi, in addition to other storage systems-related responsibilities. He received his B.S. degree in chemistry from Yale University cum laude with distinction in the major in 1979, and his Ph.D. in inorganic chemistry from Columbia University in 1984. His thesis work included spectroscopic analyses of model compounds for the inorganic active sites of proteins. He focused his interests in spectroscopy on surface analytical techniques during postdoctoral work at the Massachusetts Institute of Technology from 1984 to 1986. In 1986 Dr. Spool joined IBM in San Jose, with responsibility for setting up a laboratory for Rutherford backscattering spectrometry. At this time he also became a member of the American Vacuum Society. In 1988 and 1989 he taught the course "Techniques for Surface Analysis" to students of the Berkeley Extension. Dr. Spool's efforts to bring TOF–SIMS to the San Jose facility reached fruition in 1991.